

UC Berkeley

Research Reports

Title

Automated Truck Platoon Control

Permalink

<https://escholarship.org/uc/item/7c55g2qs>

Authors

Lu, Xiao-Yun
Shladover, Steven E

Publication Date

2011-06-01

**CALIFORNIA PATH PROGRAM
INSTITUTE OF TRANSPORTATION STUDIES
UNIVERSITY OF CALIFORNIA, BERKELEY**

Automated Truck Platoon Control

Xiao-Yun Lu and Steven E. Shladover

California PATH Research Report

UCB-ITS-PRR-2011-13

Disclaimer

This document is disseminated in the interest of information exchange. The contents of this report reflect the views of the authors who are responsible for the facts and accuracy of the data presented herein. The contents do not necessarily reflect the official views or policies of the State of California. This publication does not constitute a standard, specification or regulation. This report does not constitute an endorsement by the Department of any product described herein. For individuals with sensory disabilities, this document is available in Braille, large print, audiocassette, or compact disk. To obtain a copy of this document in one of these alternate formats, please contact: the Division of Research and Innovation, MS-83, California Department of Transportation, P.O. Box 942873, Sacramento, CA 94273-0001.

June 2011

CALIFORNIA PARTNERS FOR ADVANCED TRANSPORTATION TECHNOLOGY

Report Submitted Under Cooperative Agreement DTFH61-07-H-00038

Automated Truck Platoon Control

Xiao-Yun Lu and Steven E. Shladover

California PATH Program

Institute of Transportation Studies

University of California, Berkeley

June 2011

Automated Truck Platoon Control

Abstract

This report shows a successful application of 5.9 GHz DSRC with 100 ms update intervals to coordinate the automatic longitudinal control of a platoon of three Class 8 tractor-trailer trucks. The trucks were tested not only in constant-speed cruising conditions, but also through acceleration and deceleration profiles, up and down grades, and in platoon join and split maneuvers using the DSRC coordination. These tests showed acceptable vehicle following accuracy, ride quality and platoon stability. The gaps between the trucks were varied between 10 m and 4 m to evaluate the effects of aerodynamic drag reductions on fuel savings. The most complete set of drag data, at the 6 m gap, showed fuel savings of about 4-5% for the lead truck and in the range of 10% to 14% for the following trucks. The effects of platoon gap variations between 10 m and 4 m were more difficult to determine with certainty because strong ambient winds during those tests led to large differences in the results depending on the truck direction of travel, but the results imply a significant potential for larger savings at the shorter gaps.

Preface

This report describes the work under the subject Cooperative Agreement that addressed automated truck platoon control, incorporating several of the deliverables that were defined in the project work plan:

- (4) Report describing expected ability of DSRC communications to support requirements for automated truck platoon control
- (9) Report on experimental performance of two-truck and three-truck automated platoons based on high-speed testing
- (11) Report on maneuvering capabilities of three-truck platoon control system.

This report is organized in six sections:

1. Using DSRC in Automated Truck Control (specifically addressing Deliverable (4))
2. Design, Implementation and Testing of Automated Truck Platoon
3. Maneuver Capability of Automated Trucks (specifically addressing Deliverable (11))
4. Fault Detection and Handling
5. Fuel Economy Analysis
6. Concluding Remarks

1. Using DSRC (Dedicated Short Range Communication) in Automated Truck Platoon Longitudinal Control

For automated vehicle platooning, reliable inter-vehicle communication is essential to maintain string stability. The data packets passed between vehicles are less than 200 bytes, which is rather small. It is required that the communication be bi-directional.

In this project, two 5.9 GHz DSRC radio sets have been evaluated, the Savari Onboard Unit (SOBU), and the Denso Wireless Safety Unit (WSU), seen in the photographs in Figure 1.1. The SOBU was first used for truck platoon control from 2008, when it was tested at low speed at the PATH test track at the University of California Richmond Field Station (RFS). It was also used for high speed truck platooning in September 2010 on Nevada SR722 near Austin, Nevada. In that test, a standard single antenna was used for all three trucks. With 53 ft trailers hauled by the truck tractors, the system was generally able to maintain communication among three trucks, but if the three trucks were lined up precisely, some communication drops were observed. (For our application, we define a communication error as packet drops for 20 consecutive steps. At a 10 Hz update rate, this means the signal would be dropped continuously for 2 s.) In the September platooning test, we intentionally drove the middle truck slightly to the right side of the other trucks, with about 1 ft lateral offset, to prevent it from blocking line of sight signal transmission between the first and last trucks. This lateral offset is believed to have adversely affected the aerodynamic drag characteristics and the corresponding fuel economy results.



Figure 1.1. Two DSRC Radio sets that were tested

We planned to complete the May 2011 three-truck highway speed tests using the Denso WSU radios for vehicle-vehicle communication because these radios were designed to support diversity, enabling antennas to be mounted on both side mirrors of each truck. With this arrangement, the antennas should always be able to maintain line of sight connections among all three trucks, so that the trucks could be driven well aligned with each other. This would enable us to more accurately measure the fuel consumption savings that can be achieved as a function of truck following gap.

We developed interfaces and device drivers for the Denso WSU unit using a similar communication protocol as with the SOBU. The WSU units were then successfully tested at RFS with three tractors since we did not have long trailers at that stage.

In the highway speed tests conducted in May 2011, the Denso WSU units were first tried in the belief that they would provide more reliable communication between trucks. However, with the combined tractor and trailer configuration, the Denso WSU units could barely achieve the initial hand-shakes among the three trucks. Although they worked properly for two trucks, they were never successfully used for three trucks in the Nevada tests. This forced us to return to the SOBU units with a single higher gain antenna, which is longer than the original antenna, and with the middle truck driven with a lateral offset relative to the others. With this antenna and lateral offset, the system worked reliably with the complete tractor and trailer configuration, which allowed us to successfully finish all the tests on SR722 near Austin, Nevada.

2. Design, Implementation and Testing of Automated Truck Platoon

2.1 Development of Automated Truck Platoon

In order to demonstrate the viability of the automated truck platoon concept, it was necessary to show that the platoon could be operated under a realistic range of operating conditions, not just under the simplest or most ideal conditions. The required operating conditions including not only steady-state cruising at a constant speed, but also speed changes, platoon join and split maneuvers and ascending and descending highway grades.

The most challenging maneuver is platooning up/down a grade because the truck has very limited torque available for maneuvering at higher speeds due to its low power-to-mass ratio. The limited torque has to be used for both distance and speed control, as well as overcoming the grade going up a hill. Considering that the electronic braking systems (EBS) did not function as expected for two of the three trucks, platooning going down a grade was also challenging. To overcome this difficulty, we developed a combined brake system control strategy integrating three braking systems: engine brake, transmission retarder and air brake. It turned out that the combination of engine brake and transmission retarder could provide adequate braking torque so that the air brake was only necessary in the following cases: (a) emergency stop, and (b) braking to stop at very low speed (<8 mph). When the ambient and engine temperatures were high during testing, the engine fan had to be used, which alone draws 10% of the engine power, producing a large disturbance to the control system. This happened often during the tests.

2.2 Truck System Modeling and Control System Structure

Truck system modeling for control design in this project evolved from that developed in 2003. Detailed modeling of each component is referred to [1, 7]. The overall system modeling and control system structure is depicted in Figure 2.1.

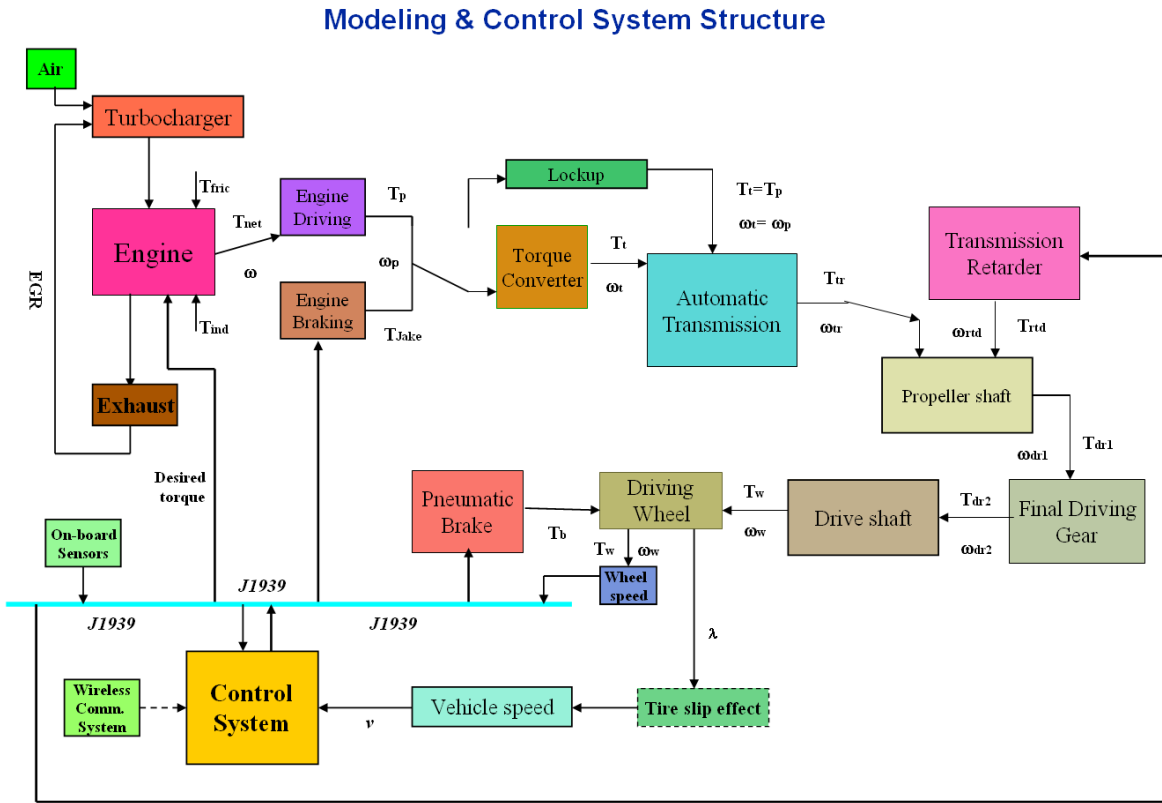


Figure 2.1 Truck System Modeling, and Sensor Reading and Control System

The control system structure and implementation were described in [3, 5, 6, 7].

The truck drivetrain model used for longitudinal control design is the same as that developed in 2003 in [1, 3, 5].

Follow the power flow in Fig. 2.1 and notice the following relationships

$$\omega_w = \omega_{dr2} = \frac{v}{h_r}$$

$$\omega_{tr} = \omega_{dr1} = \frac{v}{h_r} r_d$$

$$\omega = \omega_i = \frac{v}{h_r} r_d r_g$$

Longitudinal vehicle dynamics are obtained as

$$a = \dot{v} = \frac{r_d r_g T_{net} - (r_d T_{rtd} + T_b + F_a h_r + F_{total} h_r + M g h_r \sin \theta)}{\bar{I}} \quad (2.1)$$

$$\bar{I} = r_d^2 r_g^2 \frac{I_e}{h_r} + r_d^2 \frac{I_{tr}}{h_r} + r_d^2 \frac{I_{dr1}}{h_r} + \frac{I_{dr2}}{h_r} + \frac{I_w}{h_r} + M h_r$$

where

$$F_a = 0.5 C_a \rho_{air} A V_a^2$$

T_b and F_{total} will be modeled separately.

Engine Braking Mode: $T_{net} = -T_{jake}$ ($Jake = 0, 2, 4, 6$) is used in (2.1);

Transmission Retarder Mode: $T_{net} = 0$ in (2.1);

where

M – vehicle mass

ω – engine speed

ω_{idle} – engine idle speed

ω_p – torque converter pump speed, $\omega_p = \omega$

ω_i – torque converter turbine speed

ω_{tb} – turbocharger speed

ω_{tr} – transmission output speed

ω_{dr1} – propeller-shaft speed including front part of final gear

ω_{dr2} – drive-shaft speed including front rear of final gear, final drive end

ω_{dr} – drive-line speed (considered as lump sum), at final drive end

ω_w – wheel angular speed

v – vehicle wheel speed (longitudinal) is used for all control design

a – acceleration

α_f – fueling rate

I_e – engine inertia

I_{tr} – transmission inertia

I_{dr1} – drive line inertia (before final gear)

I_{dr2} – drive line inertia (after final gear)

I_{dr} – lump sum drive line inertia ($I_{dr} = I_{dr1} + I_{dr2}$)

I_w – wheel inertia

P_m – intake manifold pressure or *turbocharger booster pressure*

T_d – drive-line torque loss

T_{ind} – engine indicated torque

T_{net} – engine net output torque

T_p – torque converter pump torque, $T_p = T_{net}$

T_t – torque converter turbine torque

T_b – service brake torque

T_{jake} – engine brake torque

T_{tr} – transmission output torque

T_{dr1} – final gear input torque (or equivalently propeller shaft final end torque)

T_{dr2} – final gear output torque

T_w – engine torque passed to wheel

T_{rtd} – transmission retarder torque

T_{fric} – engine friction torque

T_{e_brk} – engine braking effect torque when $T_{net} < T_{net_des}$

F_a – aerodynamic resistance force

F_r – rolling resistance force

F_f – friction force

$F_{eng-brk}$ – engine braking force transmitted to wheels when throttle is released

$F_{total} = F_r + F_{eng-brk}$

F_o – engine brake force when clutch is engaged and fueling is at idle

h_r – effective tire radius

θ – road grade, $\theta > 0$ means ascending

r_g – transmission gear ratio

r_d – final-drive gear ratio

R_g – gear ratio $R_g = r_g r_d$, $\omega_t = \frac{v R_g}{h_r}$

V_a – relative speed of the truck to the ambient air in the longitudinal direction (it is the vehicle speed if there is no wind)

ρ_{air} – air density

2.3 Sensors and Actuators

As depicted in Figure 2.1, most vehicle information is obtained through the truck's internal J1939 data bus. Engine control is based on the built –in torque control of the engine control

system. Brake system control includes three parts: Engine compression brake (Jake brake), transmission retarder, and pneumatic brake. Their control actuations are also realized through the J1939 bus.



Figure 2.2 Sensors and Actuators Installed on Three Trucks

Each truck was equipped with an EVT-300 Doppler radar by Freightliner – the manufacturer of the trucks. The Gold truck also had a DENSO lidar, which has an azimuthal scanning capability. The Silver Truck was equipped with a single beam MDL lidar, which has no scanning capability. The full complement of sensors and actuators on the trucks is shown in Figure 2.2.

2.4 Practical String Stability for Vehicle Platooning

As discussed in detail in [4], practical string stability in automated vehicle platooning needs to take into account the following factors in practice:

- Time lags in sensors and actuators;
- Pure time delays in sensor measurement and signal processing;
- Model mismatches;

- Measurement noise;
- External disturbances from the environment, including the road and wind.

Without those factors, one could achieve asymptotic string stability – tracking errors diminish from the platoon head to the end. In such an ideal case, one could talk about a platoon of arbitrary length (number of vehicles). However, with the aforementioned factors taken into account, the situation is quite different: the platoon length is limited by the following factors:

- The bandwidth of the feedback control on each vehicle;
- The total time delay accumulated from the leader to the last follower of the platoon;
- The internal and external disturbances accumulated along the platoon.

In general, the larger the accumulated time delay and disturbances, the shorter the platoon that could be formed and maintained; and the larger the control bandwidth, the longer the platoon that could be achieved.

2.5 Field Tests

The first set of high-speed highway tests of the three-truck platoon were conducted on Nevada SR-722, to the west side of Austin, NV, in September 2010. This is a straight, flat, section of two-lane highway with such a low daily traffic volume (AADT 60 vehicles) that it was practical for Nevada DOT to temporarily close it during each individual test run.

We investigated several test sites for the final set of high-speed tests of the three-truck platoon, including the dry lake bed at Edwards Air Force Base and two lightly-traveled highways in Nevada. The Edwards Air Force Base site is perfectly flat (so we can't test driving on grades) and is covered with very fine dust, which was expected to create visibility problems for the lidar sensors when it is stirred up by the truck tires. We visited the two Nevada sites, and discovered that the initially preferred site on SR-121 did not have suitable locations for turning the trucks around at the end of each test run. This led to a preference for a return to SR-722, where we did the first round of testing, with an extension to an additional section further to the west of the original site, where we could do some testing on grades.

The truck control computer systems were modified by changing from a “mechanical hard drive” to a “solid state hard drive” with the same real-time operating system QNX 4.1. The objective for this change was to avoid vibration-caused computer rebooting during the test runs, which happened in the September 2010 tests in Nevada. Some preliminary tests were conducted for static and real-time runs at RFS using the solid state drives. However, the new solid state drives caused the operating systems to lock up on the PC-104 computers, which would be a serious problem if it occurred during high speed tests. To solve this problem, we returned to the original mechanical hard disk and remounted the PC-104 horizontally with four air suspensions as shock

absorbers, as shown in Figure 2.3. With this hardware setup, the three PC-104 computers ran reliably during the tests in May 2011 in Nevada.

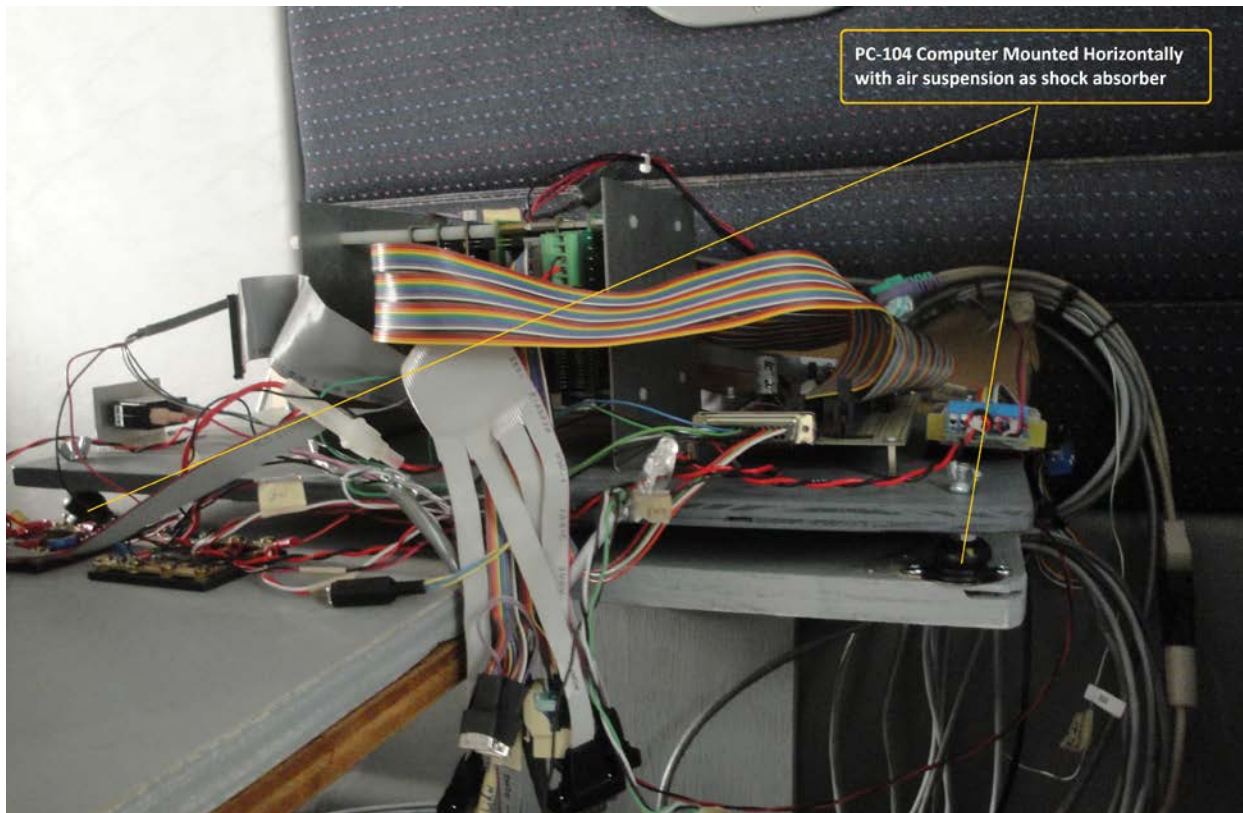


Figure 2.3 PC-104 computer stack mounted horizontally with four air suspensions as the shock absorbers

The roadway section marked in red on SR-722 in Nevada in Figure 2.4 is almost flat. It was used for tests in September 2010 and May 2011. In the tests conducted in September 2010, the main objective was to test the three-truck combination for short distance following or platooning. The shortest inter-vehicle distance achieved then was 6 m. In the May 2011 tests, besides short distance following, some fundamental maneuvers were tested, which include: simultaneously splitting/joining, individually splitting/joining, variable maximum speed for string stability tests, and ascending/descending a hill.



Figure 2.4 SR722 in Austin Nevada. The Red section is almost flat; the Blue Section contains a hill with Grade Levels A, B, and C as defined in Table 2.1.

The road grades for this section with respect to postmile are listed in Table 2.1. The three test trucks with their trailers are seen at the turnaround location at the eastern end of the test section in Figure 2.5.

Table 2.1. Road Grade of Test Section of SR722 East Bound at Austin, Nevada.

Starting Distance	Ending Distance	Total Distance	Grade	Grade Class
42.7938	43.0734	0.2796	-1.71	B
43.0734	43.2121	0.1386	-0.2	A
43.2121	46.4544	3.2423	-1.25	B
46.4544	46.5207	0.0663	-0.44	A
46.5207	46.6997	0.179	-0.59	B
46.6997	46.926	0.2263	-0.4	A
46.926	46.9503	0.0243	-0.53	B
46.9503	47.3572	0.4069	-0.36	A
47.3572	47.3716	0.0144	-0.51	B
47.3716	48.4326	1.061	-0.3	A
48.4326	48.4348	0.0022	-0.51	B
48.4348	55.7288	7.294	-0.15	A



Figure 2.5. Three Automated Trucks (Blue, Gold and Silver) with Trailers at Eastern Turning Point on SR 722, May 2011

2.6 Test Results

The following parameters have been plotted against global time to show the performance of the truck platoon control system:

- Measured speed in mph – essentially wheel speed. Since the road surface was dry during the tests, the speed could be considered as true vehicle speed;
- Maneuver ID: Maneuver ID is used to coordinate the behavior of each vehicle in a platoon and to determine a scenario which is composed of several elemental maneuvers such as: static and ready to go (ID=2); acceleration (ID=3); cruise at constant speed (ID=7); splitting platoon to follow at a longer distance (ID=8); joining platoon to follow at a shorter distance (ID=6); deceleration but not for stopping (ID=27); closed loop deceleration in preparation for a complete stop (ID=29); final open-loop braking to a complete stop (ID=30);
- Speed tracking error in m/s and distance tracking error in m;
- Radar and lidar relative distance measurements and their fusion to form a reliable estimate of inter-vehicle distance;
- For ascending and descending a hill, GPS reading and grade estimation based on GPS reading are also plotted;

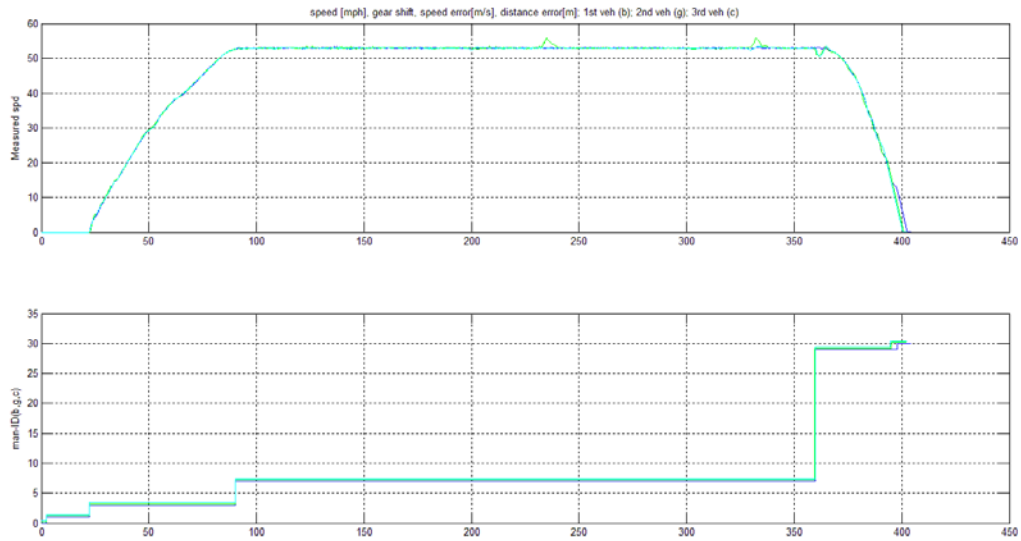


Figure 2.6a Three Trucks Platooning with 4 m inter-vehicle distance; Configuration: Blue Truck 1st, Silver Truck 2nd, and Gold Truck 3rd, speed trajectories of three trucks and their maneuver IDs

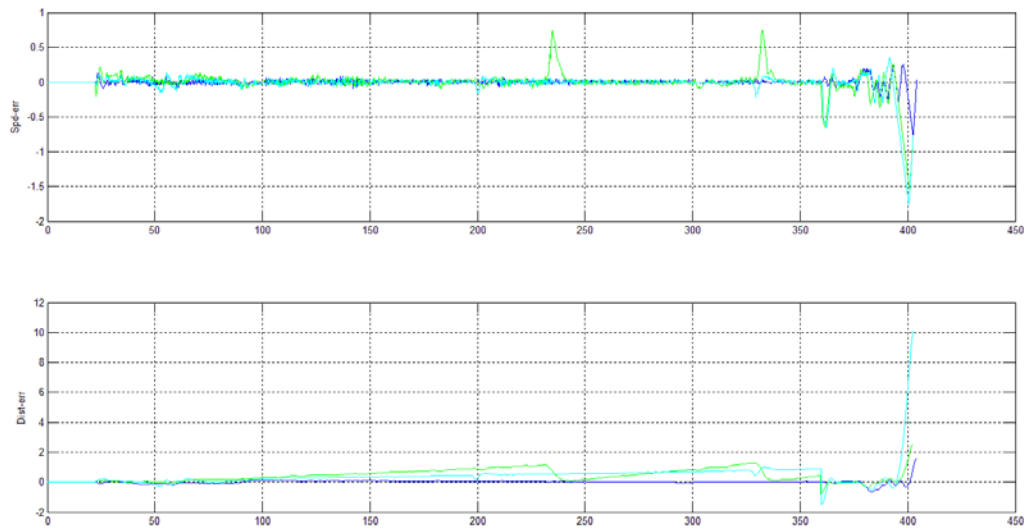


Figure 2.6b. Three Trucks Platooning with 4 m inter-vehicle distance; Configuration: Blue Truck 1st, Silver Truck 2nd, and Gold Truck 3rd: Speed and distance tracking error

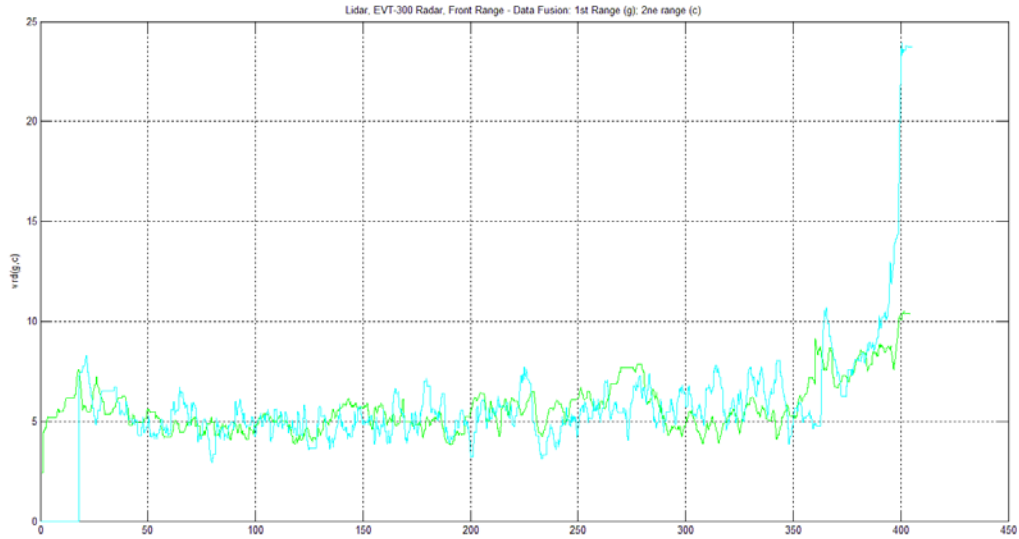


Figure 2.6c. Three Trucks Platooning with 4 m inter-vehicle distance; Configuration: Blue Truck 1st, Silver Truck 2nd, and Gold Truck 3rd : EVT-300 Radar Range Measurements

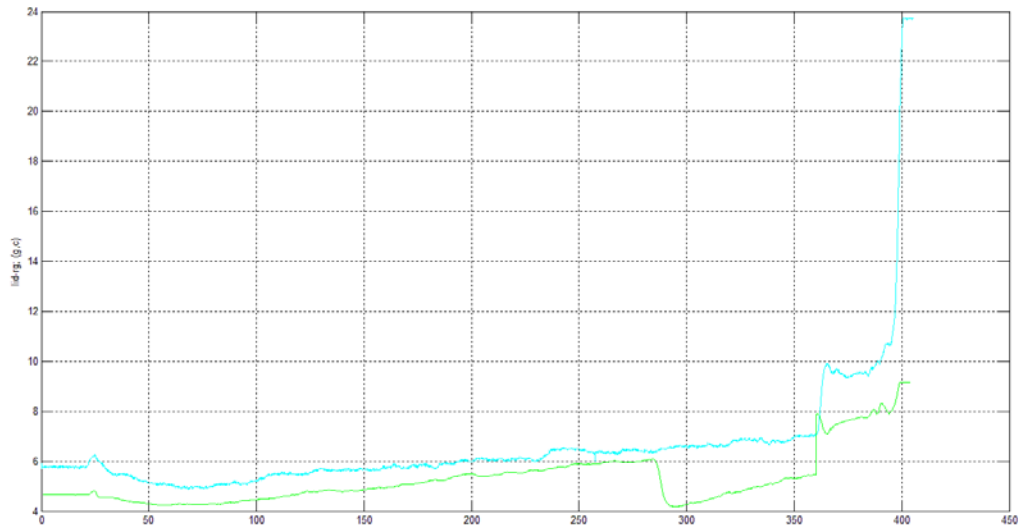


Figure 2.6d. Three Trucks Platooning with 4 m inter-vehicle distance; Configuration: Blue Truck 1st, Silver Truck 2nd, and Gold Truck 3rd : Lidar range measurement

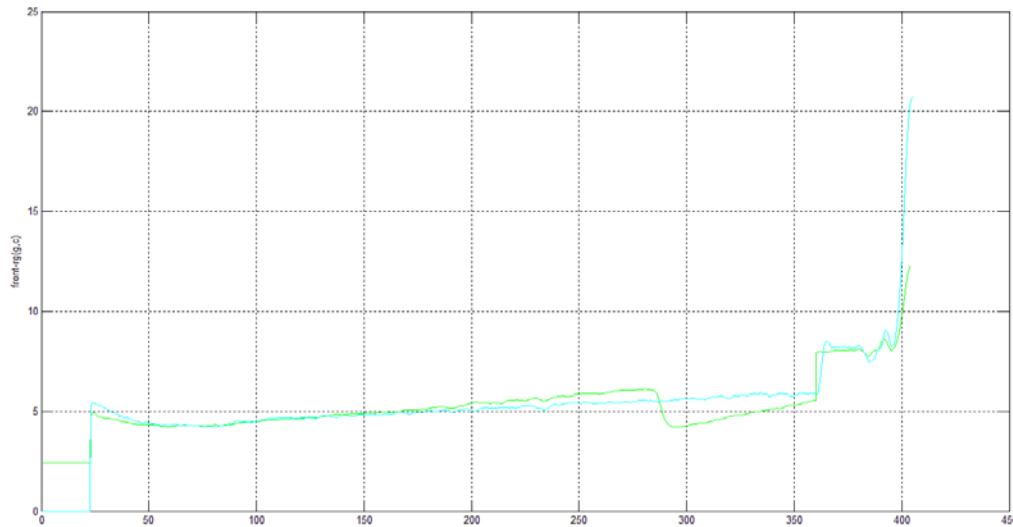


Figure 2.6e. Three Truck Platooning with 4 m target inter-vehicle distance; the drifting was due to a controller tuning problem (which did not happen to Sept. 2010 tests); Configuration: Blue Truck 1st, Silver Truck 2nd, and Gold Truck 3rd : Fused radar and lidar range measurement

For measuring the speed and distance tracking, maximum values and Root Mean Square (RMS) errors have been used to quantify the error values based on the test run data. Two configurations have been tested:

- Configuration 1: Blue Truck; Gold Truck; Silver Truck
- Configuration 2: Blue Truck; Silver Truck; Gold Truck

Using those two configurations for platooning tests has two purposes: (a) to check the robustness of the controller with respect to different configurations; (b) to conduct fuel economy analysis for different platoon configuration to exclude the possibility of bias caused by slightly different vehicle characteristics.

The following Tables 2.2 and 2.3 list the RMS and maximum errors for speed and distance tracking of the two configurations respectively. It can be observed that, for the first platoon configuration (Blue, Gold, Silver), the speed and distance tracking errors were significantly larger than for the second platoon configuration (Blue, Silver, Gold). The reason for this is that the first platoon configuration was tested earlier than the second one. Before testing the first configuration, we had communication system problems: the three DENSO WSU successfully tested at RFS stopped working in Nevada. This wasted two days of the limited field test period and forced us to go back to the SOBU unit. Due to limited field test time period, we did not have time to tune the controller adequately to address the strong winds and other factors. Instead, we relied on the controller used for tests at the same site in September 2010 for the first two trucks (Blue and Gold) and paid more attention to achieving adequate performance of the third truck (Silver) for string stability. In the test of the second configuration, the Gold truck was in the third position and its controller was re-tuned during those tests. Its performance was improved

accordingly. This ended up with the situation that the second configuration had better platooning performance than the first.

It can be observed from Table 2.2 that the maximum distance error is rather significant compared to the desired following distance for the second truck. This was in fact caused by drifting of the second truck with respect to the first truck as shown in the following Figure 2.7. From radar and lidar data, it was observed that this drift always caused a gradual increase in the separation of the second truck with respect to the first truck. This drifting error could be caused by the stiffness of the controller and in control synthesis. This is sometimes necessary for robustness of the feedback control for other maneuvers including variable maximum speed, splitting and joining, and ascending and descending a hill. The same controller performed much better in distance tracking during the tests in September 2010 on the same section of road. The only differences were: (a) the trailers were slightly different; and (2) the weather conditions in September 2010 were much better – almost no wind at all. However, the above data show that tuning the controller for a good balance between control stiffness and good response in distance control needs further consideration in the future.

After swapping the truck positions, the controller of the Gold truck was tuned to some extent. It can be observed that the distance tracking error was reduced for this configuration, when it was in the third position within the platoon. It is expected that these errors could be further reduced by tuning of the controller in future work. In the September 2010 tests at the same site, a 6 m inter-vehicle following distance was adopted for eight successful runs. The test data from those runs have been analyzed, with the speed and distance tracking errors listed in Table 2.4. It can be observed that the distance tracking error of the second truck with respect to the first for the test runs in September 2010 was not as significant as in Table 2.2, which represented tests under much windier conditions.

Table 2.2. RMS at Cruise Phase for First Platoon Configuration (Blue, Gold, Silver): Data on 05/26 and 05/27

Data number	Dir	Max spd [mph]	Des dist [m]	Blue – 1 st				Gold – 2 nd				Silver – 3 rd			
				Distance Error		Speed Error		Distance Error		Speed Error		Distance Error		Speed Error	
				RMS	Max	RMS	Max	RMS	Max	RMS	Max	RMS	Max	RMS	Max
04_07	E	53	6	0.0890	0.2076	0.0153	0.107	1.4223	3.3732	0.0264	0.1296	0.3278	1.3230	0.1183	0.5760
04_08	W	53	6	0.0935	0.2178	0.0154	0.121	1.5874	3.5232	0.0298	0.1296	0.2557	1.1358	0.0874	0.5040
04_09	E	53	6	0.0539	0.1332	0.0163	0.091	1.6944	3.5688	0.0240	0.0864	0.3774	1.3098	0.1166	0.6402
05_10	W	53	5	0.0885	0.1974	0.0158	0.092	1.8508	3.9366	0.0249	0.1152	0.2289	0.6888	0.0321	0.2160
05_11	E	53	5	0.0539	0.1338	0.0166	0.077	1.8473	3.7998	0.0248	0.1008	0.3039	1.2498	0.0723	0.5112
05_12	W	53	5	0.0971	0.2712	0.0156	0.092	1.1533	2.8404	0.0274	0.1584	0.2063	0.4302	0.0295	0.1584
05_13	E	53	5	0.0463	0.1032	0.0152	0.081	1.7840	3.7992	0.0232	0.1296	0.2363	0.6558	0.0471	0.3672
06_14	W	53	4	0.0847	0.2220	0.0174	0.092	2.6512	5.1276	0.0210	0.1008	0.4153	0.6846	0.0275	0.1728
06_15	E	53	4	0.0504	0.1146	0.0153	0.096	2.1698	4.3980	0.0251	0.1008	0.1759	0.4350	0.0263	0.1512
06_3		53	4	0.0372	0.0942	0.0172	0.095	2.3726	5.1744	0.0428	0.5040	0.1741	0.7284	0.0454	0.2376
06_4		53	4	0.0864	0.1896	0.0149	0.078	2.2259	4.4700	0.0234	0.1008	0.2206	0.9894	0.0764	0.4752
06_5		53	4	0.0334	0.0804	0.0154	0.095	1.9798	4.2390	0.0332	0.4032	0.1890	1.0518	0.0687	0.3966
Mean				0.068	0.164	0.016	0.093	1.895	4.021	0.027	0.172	0.259	0.890	0.062	0.367

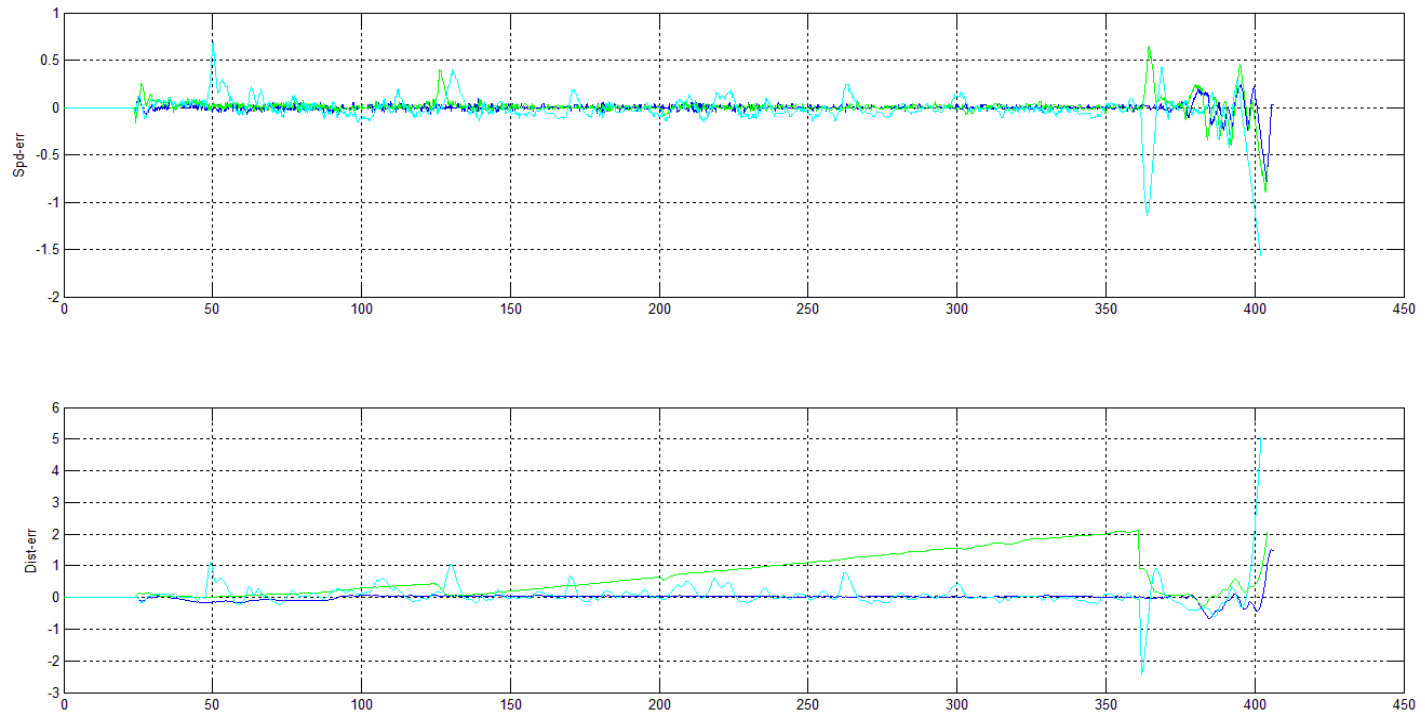


Figure 2.7. The large tracking distance error was caused by drifting of the second truck with respect to the first truck

Table 2.3. RMS and Maximum Tracking Error at Cruise Phase for Second Platoon Configuration Blue, Silver, Gold

Data number	Dir	Max spd [mph]	Des dist [m]	Blue – 1 st				Silver – 2 nd				Gold – 3 rd			
				Distance Error		Speed Error		Distance Error		Speed Error		Distance Error		Speed Error	
				RMS	Max	RMS	Max	RMS	Max	RMS	Max	RMS	Max	RMS	Max
02_10	W	53	8	0.0961	0.2592	0.0148	0.1212	0.1419	0.7662	0.0344	0.2880	0.6034	1.6830	0.0285	0.1296
02_11	E	53	8	0.0340	0.0972	0.0145	0.0810	0.1900	1.0062	0.0762	0.5256	0.5068	1.1142	0.0491	0.2160
02_12	W	53	8	0.0861	0.2052	0.0149	0.0924	0.1537	1.0236	0.0514	0.4896	1.0835	2.6700	0.0373	0.2016
02_13	E	53	8	0.0440	0.1482	0.0164	0.0918	0.1444	0.9000	0.0646	0.4896	1.2655	3.0306	0.0904	0.9648
03_14	W	53	7	0.0948	0.2202	0.0154	0.0924	0.0745	0.3648	0.0306	0.2304	0.5140	1.5456	0.0319	0.1296
03_15	E	53	7	0.0551	0.1080	0.0151	0.0768	0.1651	0.4758	0.0276	0.2232	1.4319	3.1602	0.0264	0.1152
04_16	W	53	6	0.1012	0.2718	0.0163	0.0924	0.2742	0.5910	0.0255	0.1296	1.2712	2.7798	0.0681	0.7632
04_17	E	53	6	0.0498	0.1170	0.0141	0.0768	0.0780	0.5046	0.0277	0.2592	0.9201	2.1312	0.0614	0.7200
05_18	W	53	5	0.0995	0.2328	0.0165	0.0924	0.4403	0.8640	0.0205	0.1008	2.5364	4.8180	0.1147	1.1952
05_19	E	53	5	0.0550	0.1386	0.0154	0.0912	0.4869	0.9966	0.0243	0.2160	1.2082	2.5224	0.0861	0.7488
06_20	W	53	4	0.0941	0.2244	0.0155	0.0924	0.6458	1.1628	0.0201	0.1008	1.6121	3.1680	0.0777	0.8928
06_21	E	53	4	0.0584	0.1392	0.0148	0.0906	0.7853	1.5942	0.0284	0.3378	1.6153	3.9762	0.0713	0.6624
Mean				0.0723	0.1802	0.0153	0.0910	0.2983	0.8542	0.0359	0.2826	1.2140	2.7166	0.0619	0.5616

Table 2.4. Speed and distance tracking error (RMS and Max) for tests in September 2010

Data number	Dir	Max spd [mph]	Des dist [m]	Blue – 1 st				Gold – 2 nd				Silver – 3 rd			
				Distance Error		Speed Error		Distance Error		Speed Error		Distance Error		Speed Error	
				RMS	Max	RMS	Max	RMS	Max	RMS	Max	RMS	Max	RMS	Max
1	W	53	6	0.1197	0.2910	0.0271	0.1550	0.9388	1.6170	0.0703	0.2880	0.4392	1.0960	0.0922	0.3840
2	E	53	6	0.0953	0.2450	0.0228	0.1110	0.7998	1.4360	0.0597	0.2160	0.3827	1.0110	0.0840	0.3360
3	W	53	6	0.1183	0.2790	0.0256	0.1550	0.4195	1.0250	0.0687	0.2640	0.5508	1.2500	0.0903	0.3600
4	E	53	6	0.0809	0.2010	0.0245	0.1350	0.8375	1.5140	1.5140	0.2400	0.4275	0.9750	0.0690	0.3240
5	W	53	6	0.1219	0.3520	0.0269	0.1330	0.6610	1.2960	0.0683	0.2160	0.3332	0.8620	0.1003	0.3840
6	E	53	6	0.0840	0.2000	0.0253	0.1350	0.7712	1.4820	0.0648	0.2640	0.3280	0.9110	0.0818	0.2820
7	W	53	6	0.1202	0.3480	0.0263	0.1550	0.2525	0.6860	0.0758	0.2400	1.1738	2.0910	0.0813	0.3840
8	E	53	6	0.0784	0.2070	0.0236	0.1300	0.6287	1.2740	0.0680	0.2640	0.5488	1.1900	0.0780	0.5160
Mean		53	6	0.1023	0.2654	0.0253	0.1386	0.6636	1.2913	0.2487	0.2490	0.5230	1.1733	0.0846	0.3713

3. Maneuver Capability of Automated Trucks

3.1 Develop and Test Maneuvering of Three-Truck Platoon

The following maneuvers have been developed for three-truck platooning.

- Variable maximum speed with constant following distance
- Simultaneous splitting/joining
- Simultaneous splitting followed by simultaneous joining
- Individual splitting/joining
- Individual splitting followed by individual joining
- Preliminary fault detection and handling:
 - Level 1 faults: driver is alerted to take over control immediately;
 - Level 2 faults: trucks will split to a longer distance and continue platooning;
 - Level 3 faults: all three trucks will continue platooning unless another fault appears;
- Grading up and down a hill with Grade Levels A, B and C.

These maneuvers were tested in the following sequence:

- first tested in simulation
- implemented in real-time code and tested in static run - all the software and most hardware are running without the vehicle moving, with the clutch disengaged;
- tested at low speed at PATH RFS test track
- tested at high speed on SR722 in Austin, Nevada, in May 2011.

(1) Variable maximum speed with constant following distance:

Maximum speed for the platoon is specified as a function of location. The trajectory planning is conducted automatically based on the current speed and the desired maximum speed, while taking into account the truck acceleration/deceleration capabilities at the corresponding speed. The objective of this maneuver is to test the string stability of three trucks platooning as the platoon speed fluctuates. This maneuver was tested on a 5 mile long stretch of flat road as indicated in Figure 2.4 Red section. The following figures show the speed trajectories, speed errors, distance tracking errors and other values.

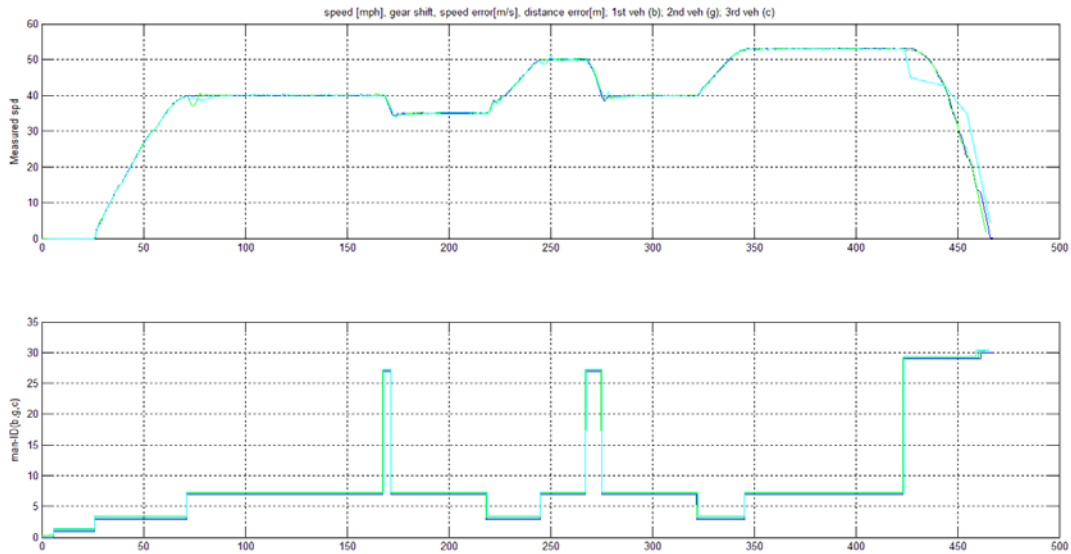


Figure 3.1 Variable Maximum Speed platooning of three trucks: measured speed trajectories, and maneuver ID; Speed changes are 0 → 40 → 35 → 50 → 40 → 53 mph

It can be observed from Figure 3.1 that the third truck started to brake earlier in the last phase – deceleration to stop. This was done on purpose as one strategy to separate the three trucks during the last phase of the maneuver. However, such strategy was replaced with a gradual separation while slowing down and finally stopping in later tested maneuvers, e.g. the platooning maneuver plotted in Figure 2.6a.

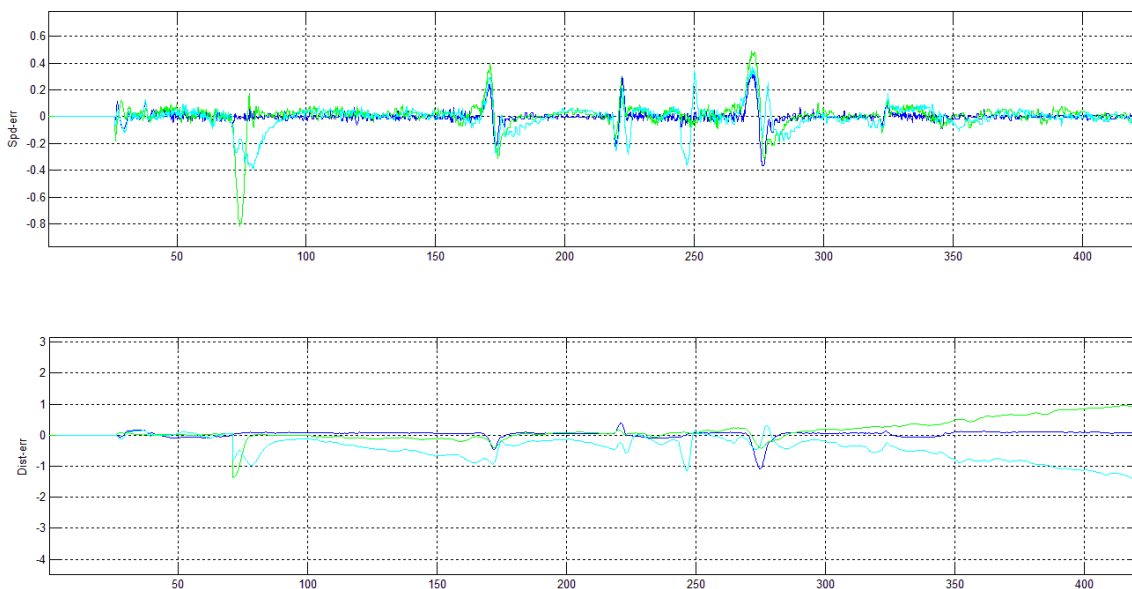


Figure 3.2 Variable Maximum Speed Platooning of Three Trucks: Speed and Distance Tracking Errors

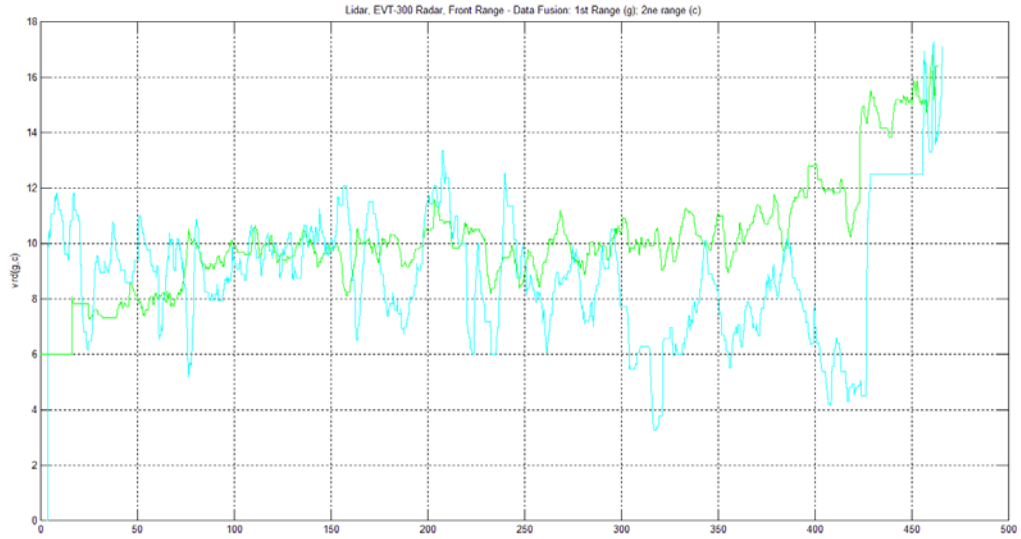


Figure 3.3. Variable Maximum Speed platooning of Three Trucks: Radar Range Measurement of Second and Third trucks

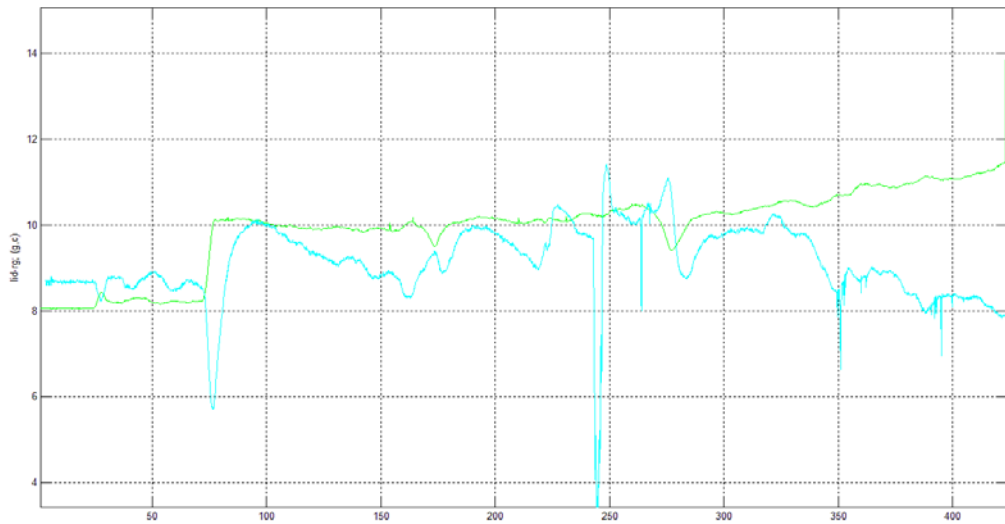


Figure 3.4 Variable Maximum Speed Platooning of Three Trucks: Lidar Range Measurement of Second and Third Trucks

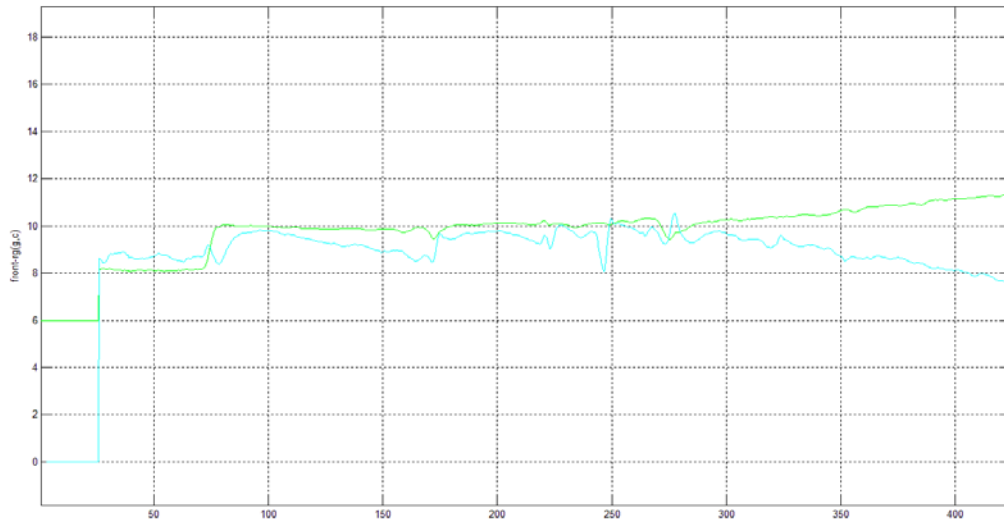


Figure 3.5 Variable Maximum Speed Platooning of Three Trucks: Fused Radar and Lidar Range Measurement of Second and Third trucks

For this maneuver, the speed and distance tracking errors are likely to amplify during speed changing phases (deceleration and acceleration except the last phase – deceleration to stop). To measure the performance, the maximum and Root Mean Square errors have been used to quantify those errors.

The following Table 3.1 presents the values of the errors for multiple runs. These results show good string stability, with the RMS errors for the third truck generally smaller than for the second truck.

Table 3.1. RMS and Maximum Errors during Acceleration and Deceleration Phases for Variable Maximum Speed with Platoon Configuration (Blue, Gold, Silver); Data from 05/23/11

#Data	Max speed change [mph]	Des distance [m]	Blue – 1 st				Gold – 2 nd				Silver – 3 rd			
			Distance Error		Speed Error		Distance Error		Speed Error		Distance Error		Speed Error	
			RMS	Max	RMS	Max	RMS	Max	RMS	Max	RMS	Max	RMS	Max
01	35; 25; 40; 30; 45	8	0.130	0.904	0.051	0.344	0.238	1.331	0.078	0.603	0.218	1.234	0.069	0.401
02	35; 25; 40; 30; 45	8	0.192	1.74	0.067	0.468	0.247	1.698	0.100	0.834	0.231	1.032	0.073	0.649
03	40; 35; 50; 40; 53	8	0.094	0.630	0.042	0.261	0.204	0.934	0.059	0.330	0.337	1.454	0.072	0.648
04	40; 35; 50; 40; 53	8	0.118	1.080	0.050	0.347	0.202	0.817	0.073	0.491	0.200	0.925	0.065	0.371
Mean			0.133	1.089	0.053	0.355	0.223	1.195	0.078	0.565	0.247	1.161	0.070	0.517

(2) Simultaneous splitting/joining:

For this maneuver, the leading truck follows its speed trajectory and virtual distance. The second and the third truck are expected to split/join from their current following distance to a new specified distance at the same time. This means that the third truck will have to split (increase inter-vehicle distance) or join (reducing inter-vehicle distance) relative to the first truck by twice as much as the second truck. After the maneuver, the inter-vehicle distances are the same.

The algorithm for splitting and joining maneuvers needs to consider the limited acceleration capability of the truck with respect to its current speed as depicted in Figure 3.6.

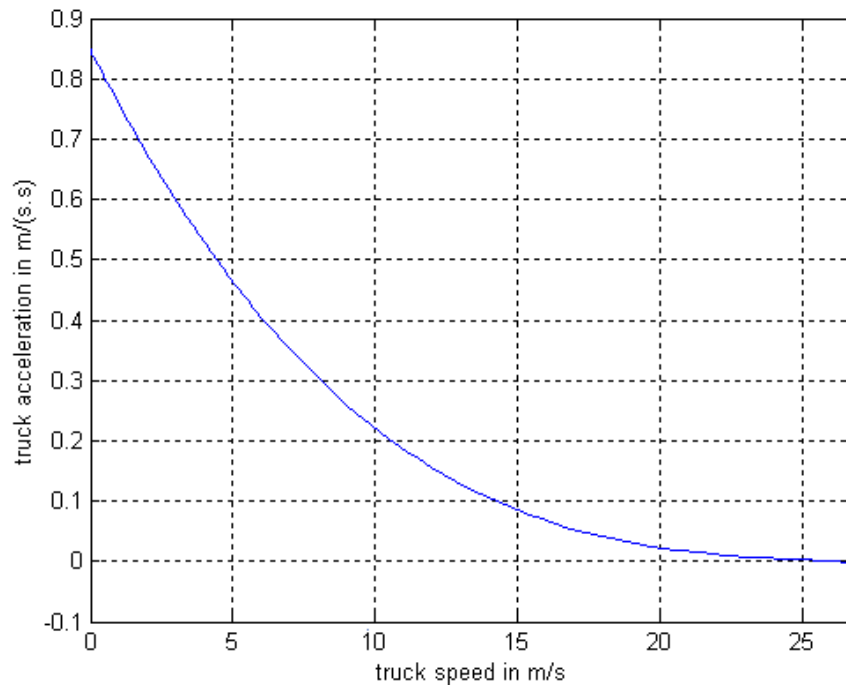


Figure 3.6. Freightliner Century Truck Acceleration Capability as a Function of Speed.

Let $A_{trk}(v(t))$ denote the curve in Figure 3.6, which is the average maximum acceleration capability of a fully loaded truck on a flat road. It depends on the vehicle speed.

The algorithm can be described based on:

- a – practical acceleration capability
- d – practical deceleration capability
- S_0 – current desired following distance
- S_f – expected desired following distance after maneuver
- $a(t)$ – vehicle acceleration during the maneuver
- $v_0(t)$ – desired speed before the maneuver
- $v_f(t)$ – desired speed after the maneuver

t_0 – maneuver start time instant

t_f – maneuver end time instant

The following discussion explains the challenges of trajectory planning: it is difficult to achieve perfect trajectory planning for both speed and distance. Suppose we are to design the speed trajectory for the joining maneuver. The speed and distance changes starting from v_0 and S_0 can be described as

$$v(t_0+kT) = \begin{cases} v_0, & k = 0 \\ v_0 + \sum_{j=1}^k a(jT) \cdot T, & k = 1, \dots, K-1 \\ v_f, & k = K \end{cases} \quad (3.1)$$

$$S(kT) = \begin{cases} S_0, & k = 0 \\ S_0 + \sum_{j=1}^k v(jT) \cdot T, & k = 1, \dots, K-1 \\ S_f, & k = K \end{cases} \quad (3.2)$$

In those discrete time descriptions, it is assumed that $a(kT)$ and $v(kT)$ are constants in the time interval $[(k-1)T, kT]$. To achieve the desired speed and distance after K time steps, the following constraints on desired acceleration and speed need to be satisfied:

$$\sum_{k=1}^K a(kT) \cdot T = v_f - v_0$$

$$\sum_{k=1}^K v(kT) \cdot T = S_f - S_0$$

which can be equivalently written as:

$$\sum_{k=1}^K a(kT) \cdot T = v_f - v_0 \quad (3.3)$$

$$\sum_{k=1}^K \left(v_0 + \sum_{j=1}^k a(jT) \cdot T \right) \cdot T = S_f - S_0$$

which is the constraints on acceleration only.

It can be observed that the trajectory planning problem for Heavy-Duty-Truck *splitting* and *joining* maneuvers can be formulated as: to find a continuous acceleration function $a(t, t)$ such that (a) the speed and distance conditions in (3.3) are jointly satisfied; and (b)

$$a(v(kT), kT) \leq A_{trk}(v(kT)), \quad k = 0, 1, \dots, K$$

Here one can assume that (v_0, v_f, S_0, S_f) are known from measurements.

It can be observed that directly solving this problem to get an exact trajectory is not trivial. To avoid those difficulties, the following approximate approach is adopted.

It is assumed that the acceleration and deceleration capability are bounded during the splitting and joining maneuvers:

$$\begin{aligned} a(t) &\leq a_{\max} \\ d(t) &\leq d_{\max} \end{aligned} \quad (3.4)$$

where a_{\max} and d_{\max} are independent of time and current vehicle speed, which are assumed to be known for now and will be determined later, and $t \in [t_0, t_0 + T_f]$ which is the time interval for maneuvering. For simplicity, it is further assumed that at the start of the joining maneuver, the vehicle is in a cruise phase, i.e., it is at a constant speed and following the front vehicle at a constant speed and it is expected to be at the same speed after the maneuver. However, this assumption is not very critical [9]. The following trajectory planning algorithm, continuous in time, is proposed:

$$a(t) = \begin{cases} 0, & t = t_0 \\ \frac{1}{2}(S_1 - S_0) \cdot \frac{\pi^2}{T_f^2} \cdot \cos[\pi(t - t_0)/T_f], & t_0 < t < t_0 + T_f \\ 0, & t \geq t_0 + T_f \end{cases}$$

$$v(t) = \begin{cases} v_0, & t = t_0 \\ v_0 + \frac{1}{2}(S_1 - S_0) \cdot \frac{\pi}{T_f} \cdot \sin[\pi(t - t_0)/T_f], & t_0 \leq t < t_0 + T_f \\ v_0, & t \geq t_0 + T_f \end{cases}$$

$$S(t) = \begin{cases} S_0, & t = t_0 \\ S_0 + v_0 t - \frac{(S_1 - S_0)}{2} (1 - \cos(\pi(t - t_0)/T_f)), & t_0 \leq t < t_0 + T_f \\ S_f, & t \geq t_0 + T_f \end{cases}$$

With this trajectory planning strategy, desired acceleration, desired speed and acceleration are compatible in the sense that:

$$\frac{dS(t)}{dt} = v(t)$$

$$\frac{dv(t)}{dt} = a(t)$$

holds for any T_f . Therefore, it is always possible to increase T_f such that the desired acceleration demand is low enough, which the engine can provide within the limited torque range indicated by Figure 3.6.

Now given desired distance after joining and the bound on acceleration capability a_{\max} , the expected joining time can be determined from the following equation:

$$a_{\max} = \frac{1}{2}(S_1 - S_0) \cdot \frac{\pi^2}{T_j^2}$$

Since the condition $a_{\max}(v(t)) \leq A_{\text{trk}}(v(t))$ needs to be satisfied, in practical implementation, we can simply add this constraint and using the measured distance instead of the final time to check if the maneuver is accomplished or not as follows:

$$a(t) = \begin{cases} 0, & S(kT) = S_0 \\ \min \left\{ \frac{1}{2}(S_f - S_0) \cdot \frac{\pi^2}{T_f^2} \cdot \cos[\pi(kT - t_0)/T_f], A_{\text{trk}}(kT) \right\}, & S_0 < S(kT) < S_f \\ 0, & S(kT) = S_f \end{cases} \quad (3.5)$$

This algorithm can always apply to splitting maneuvers because truck deceleration capability can be assumed to be constant (not depending on the current vehicle speed).

Other relevant Heavy-Duty-Truck trajectory planning is referenced to [9], where the main idea was similar but more complicated trajectory planning problems were considered.

Those two maneuvers have been tested along the 5 miles long flat stretch on SR 722 in Austin, The following figures show the parameters of one test with the splitting maneuver followed by the joining maneuver.

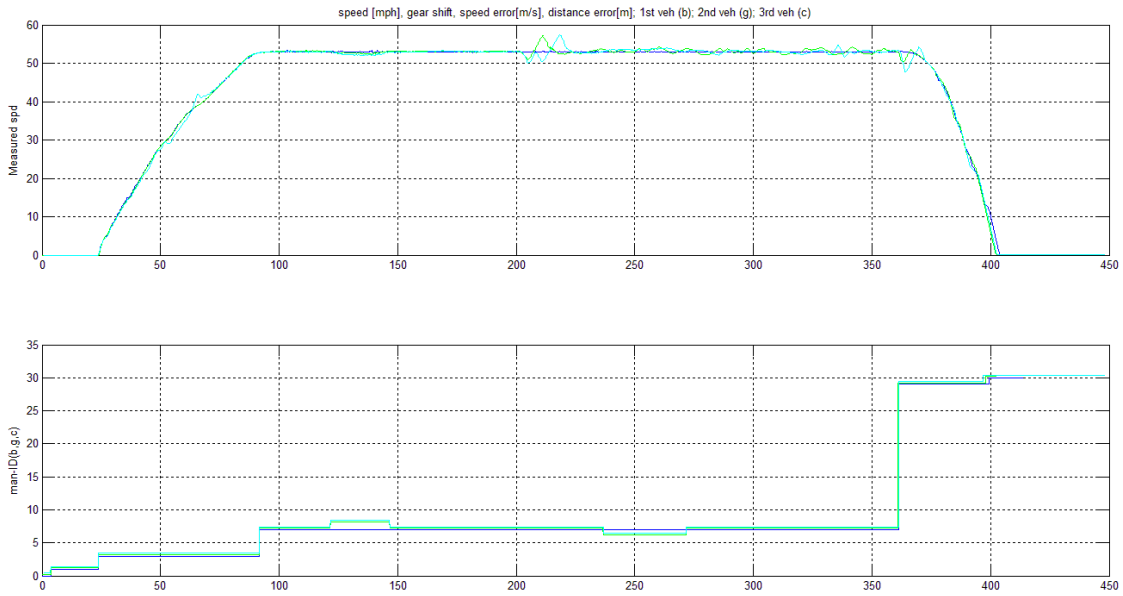


Figure 3.7. Simultaneous splitting followed by simultaneous joining for the Second and the Third truck to a pre-specified distance; after the maneuver, the inter-vehicle distances are the same; parameters plotted against time[s]: measured speed trajectories and maneuver ID values for three trucks.

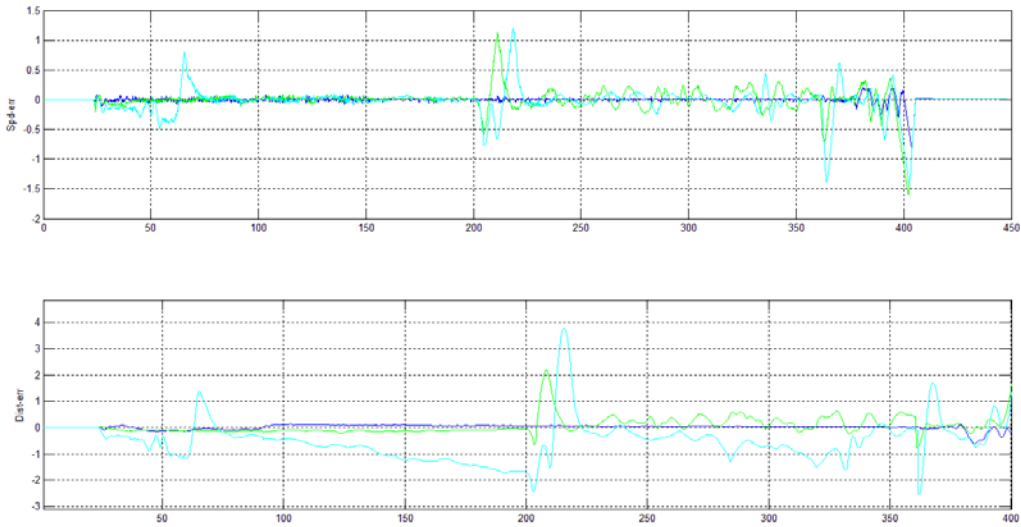


Figure 3.8. Simultaneous splitting followed by simultaneous joining for the second and the third truck to a pre-specified distance: speed and distance tracking errors.

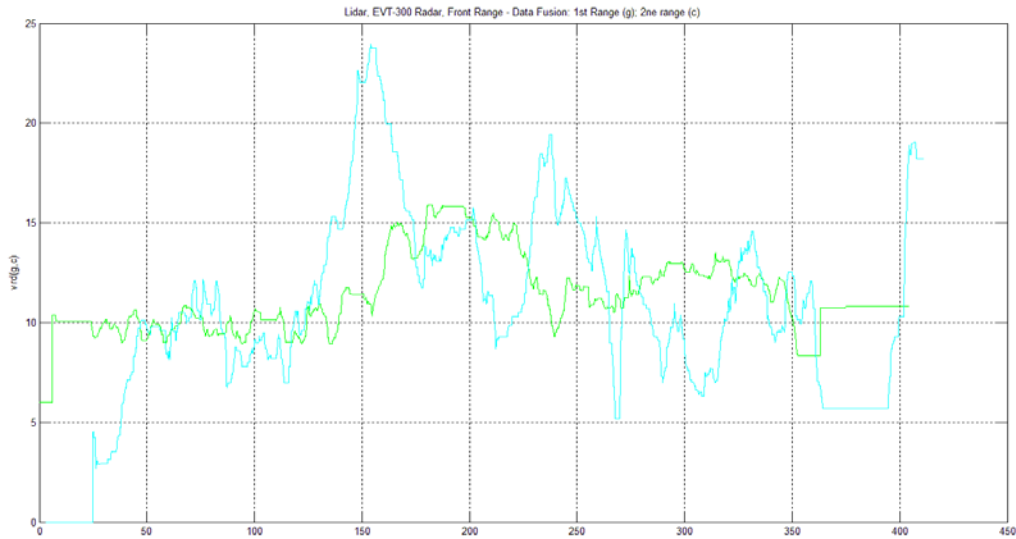


Figure 3.9. Simultaneous splitting followed by simultaneous joining for the second and the third truck to a pre-specified distance: EVT-300 Doppler radar measurement of the forward range of second and third trucks

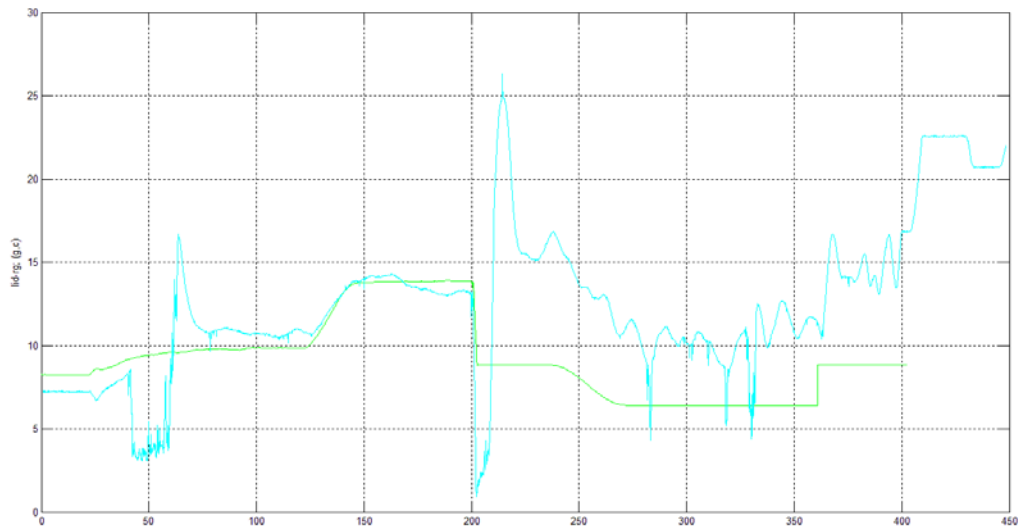


Figure 3.10. Simultaneous splitting followed by simultaneous joining for the second and the third truck to a pre-specified distance: lidar measurements of the forward range of second and third trucks

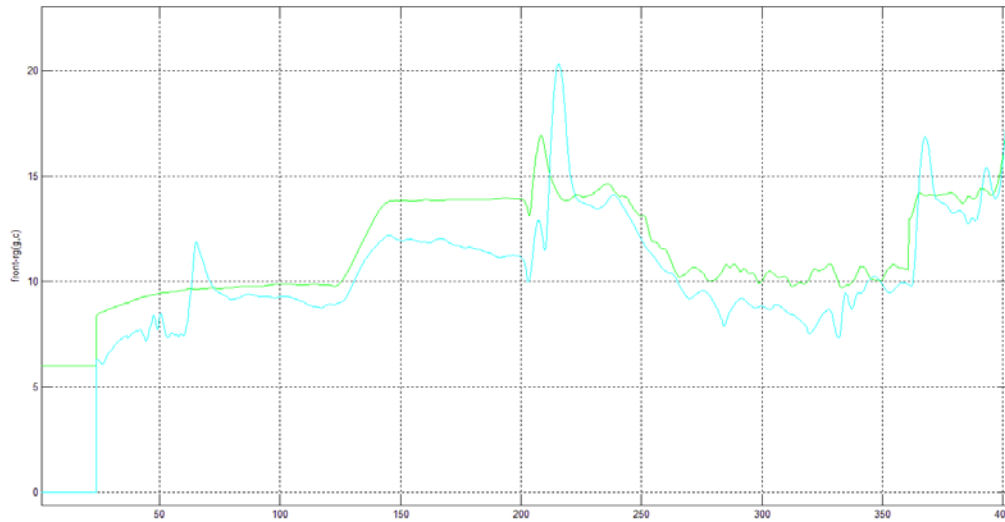


Figure 3.11. Simultaneous splitting followed by simultaneous joining for the second and the third truck to a pre-specified distance: Fused radar and lidar measurement of the forward range of second and third trucks

For those two maneuvers, the speed and distance tracking error are likely to amplify during speed changing phases (deceleration and acceleration) except the last phase – deceleration to stop. To measure the performance, the maximum and Root Mean Square errors have been used.

The following Tables 3.2 and 3.3 present the values of the errors.

Table 3.2. Error Analysis for Simultaneous Joining Maneuver: using 05/25/11 data

Data number	Max spd [mph]	Des dist [m]	Blue – 1 st				Gold – 2 nd				Silver – 3 rd			
			Distance Error		Speed Error		Distance Error		Speed Error		Distance Error		Speed Error	
			RMS	Max	RMS	Max	RMS	Max	RMS	Max	RMS	Max	RMS	Max
1	53	14→10	0.058	0.145	0.015	0.095	0.184	1.020	0.039	0.254	0.118	0.500	0.020	0.138

Table 3.3. Error Analysis for Simultaneous Splitting Maneuver: using 05/25/11 data

Data number	Max spd [mph]	Des dist [m]	Blue – 1 st				Gold – 2 nd				Silver – 3 rd			
			Distance Error		Speed Error		Distance Error		Speed Error		Distance Error		Speed Error	
			RMS	Max	RMS	Max	RMS	Max	RMS	Max	RMS	Max	RMS	Max
1	53	10→14	0.058	0.145	0.015	0.095	0.112	0.401	0.016	0.093	0.351	1.105	0.017	0.098

(3) Individual Splitting/Joining:

This maneuver is slightly different from the simultaneous splitting/joining. Although the speed trajectory planning is the same, the maneuver times and locations of the second and the third trucks are different. Obviously, for splitting, the third truck needs to maneuver first with double spaced splitting. After the completion of the third truck's split, the second truck begins to split to the desired distance. The total splitting time is 50 s and the total joining time is 70 s. After the maneuver, the distances between the first and the second trucks and between the second and the third trucks are the same. The following figures show the speed trajectory measured, trajectory planning and other parameters for the second and the third truck. Note that during the maneuver, the leading truck keeps constant speed cruising.

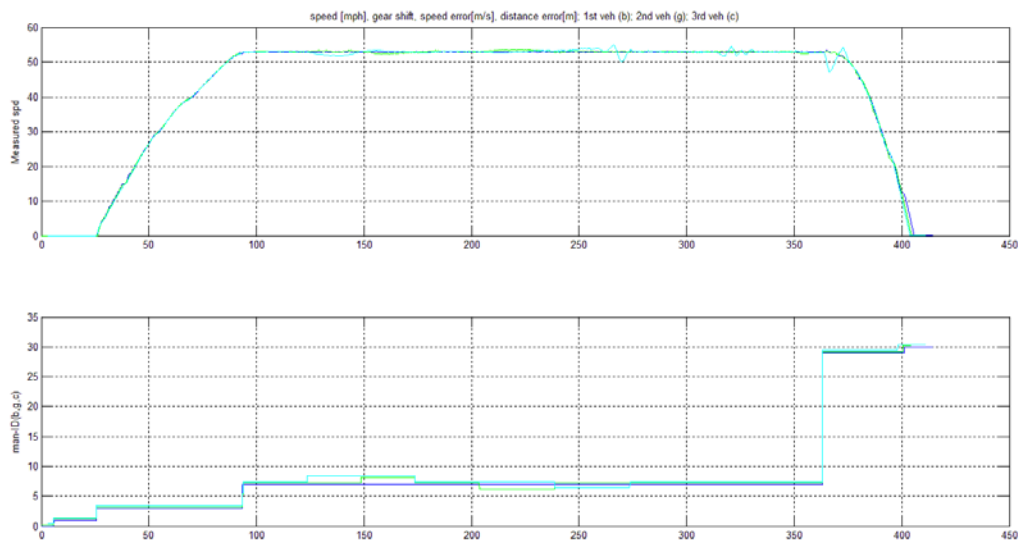


Figure 3.12. Individual splitting followed by individual joining; after each maneuver, the inter-vehicle distances are the same. Parameters plotted: measured speed trajectories and maneuver IDs for three trucks

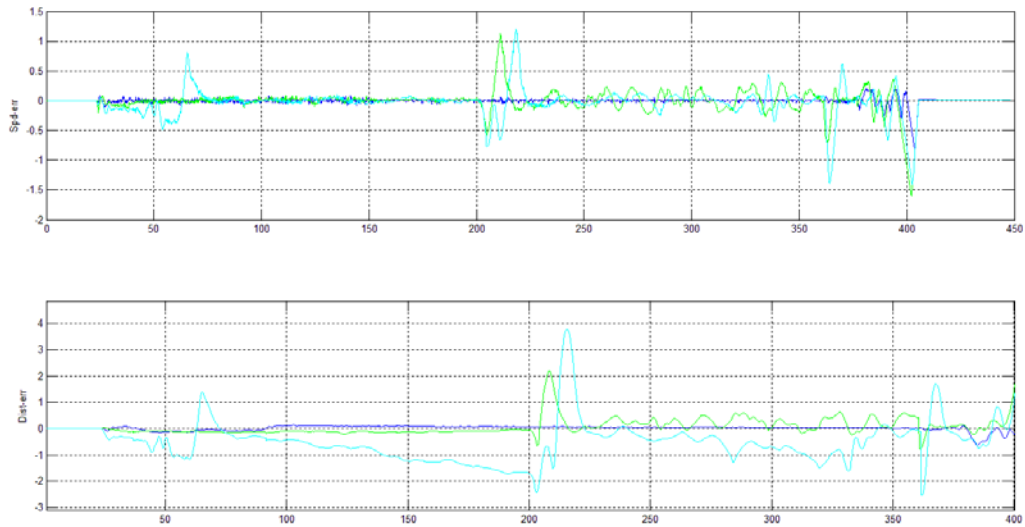


Figure 3.13. Individual splitting followed by individual joining; after each maneuver, the inter-vehicle distances are the same. Parameters plotted: Speed and Distance trajectory tracking errors

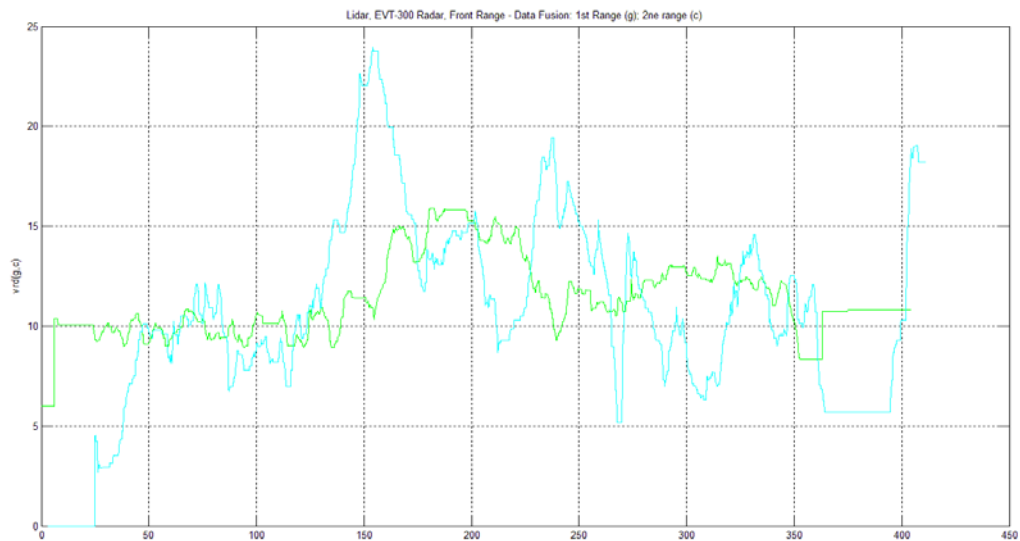


Figure 3.14. Individual splitting followed by individual joining; after each maneuver, the inter-vehicle distances are the same. Parameters plotted: EVT-300 radar measurements of the forward range of second and third trucks

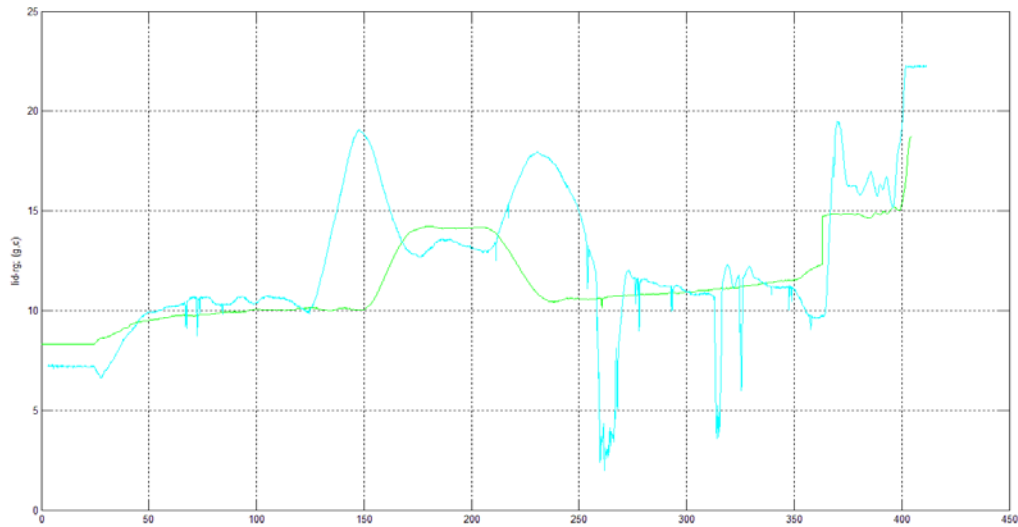


Figure 3.15. Individual splitting followed by individual joining; after each maneuver, the inter-vehicle distances are the same. Parameters plotted: Lidar measurements of the forward range of second and third trucks

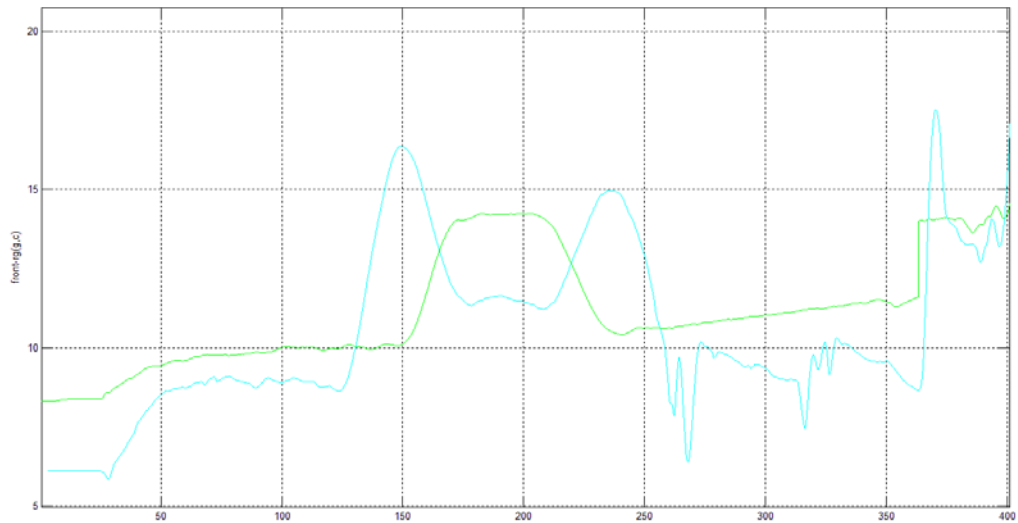


Figure 3.16. Individual splitting followed by individual joining; after each maneuver, the inter-vehicle distances are the same. Parameters plotted: fused forward ranges of second and third trucks with respect to their immediate predecessors

Similarly, for those two maneuvers, the speed and distance tracking errors are likely to amplify during speed changing phases (deceleration and acceleration) except the last phase – deceleration to stop. To measure the performance, the maximum and Root Mean Square errors have been used as shown in Tables 3.4 and 3.5.

Table 3.4. Error Analysis for Individual Splitting Maneuver: using 05/25/11 data

Data number	Max spd [mph]	Des dist [m]	Blue – 1 st				Gold – 2 nd				Silver – 3 rd			
			Distance Error		Speed Error		Distance Error		Speed Error		Distance Error		Speed Error	
			RMS	Max	RMS	Max	RMS	Max	RMS	Max	RMS	Max	RMS	Max
01	53	10→14	0.069	0.167	0.017	0.122	0.037	0.147	0.008	0.050	0.565	1.438	0.022	0.100
02	53	10→14	0.055	0.129	0.018	0.110	0.041	0.168	0.009	0.053	0.273	0.895	0.019	0.094
Mean			0.062	0.148	0.018	0.116	0.039	0.156	0.009	0.052	0.419	1.167	0.021	0.097

Table 3.5. Error Analysis for Individual Joining Maneuver: using 05/25/11 data

Data number	Max spd [mph]	Des dist [m]	Blue – 1 st				Gold – 2 nd				Silver – 3 rd			
			Distance Error		Speed Error		Distance Error		Speed Error		Distance Error		Speed Error	
			RMS	Max	RMS	Max	RMS	Max	RMS	Max	RMS	Max	RMS	Max
01	53	14→10	0.068	0.167	0.017	0.122	0.229	0.722	0.015	0.096	0.676	2.506	0.086	0.808
02	53	14→10	0.055	0.129	0.018	0.110	0.199	0.644	0.014	0.100	0.165	0.720	0.011	0.077
Mean			0.062	0.148	0.018	0.116	0.214	0.683	0.015	0.098	0.420	1.613	0.049	0.443

(4) Grading up and down a hill.

Road grade is an extra challenge to Heavy-Duty-Truck (HDT) platooning, particularly at higher speeds. As indicated before, truck acceleration/deceleration capability decreases significantly as speed increases even on a flat road. This is partly because a HDT has a very low power to weight ratio. As an example, the Freightliner Class 8 truck used in our tests has only 435 horsepower. Besides, if the engine cooling fan is switched on due to engine temperature rise, 10% of this horsepower is drawn. Therefore, longitudinal control design for platooning, which involves both speed control and distance control, must consider this serious limit. This means that, for ascending a hill, in addition to the power used to climb the road grade, enough horsepower needs to be reserved to address the speed tracking and distance tracking errors. For the preliminary test, the highest road grade is Level B as indicated in Table 3.6.

Table 3.6. Grades of the road section used for 3-truck platoon ascending/descending maneuver

Starting milepost	Ending milepost	Section Length	Grade (%)	
42.7938	43.0734	0.2796	-1.71	B
43.0734	43.2121	0.1386	-0.2	A
43.2121	46.4544	3.2423	-1.25	B
46.4544	46.5207	0.0663	-0.44	A
46.5207	46.6997	0.179	-0.59	B
46.6997	46.926	0.2263	-0.4	A
46.926	46.9503	0.0243	-0.53	B

From the model in Equation (2.1), due to the term $Mgh_r \sin \theta$ on the right hand side and the large mass M , a small road grade angle θ requires a large driving torque. Such a large torque demand cannot be simply considered as a disturbance in control design. Instead, it should be directly modeled and compensated for, which requires the real-time estimation of the current road grade for each vehicle. This has been achieved by mounting a 5 Hz GPS on each truck. By referencing the GPS location coordinate, the corresponding road grade is determined robustly through a look-up table.

The following figures show performance on the road grades.

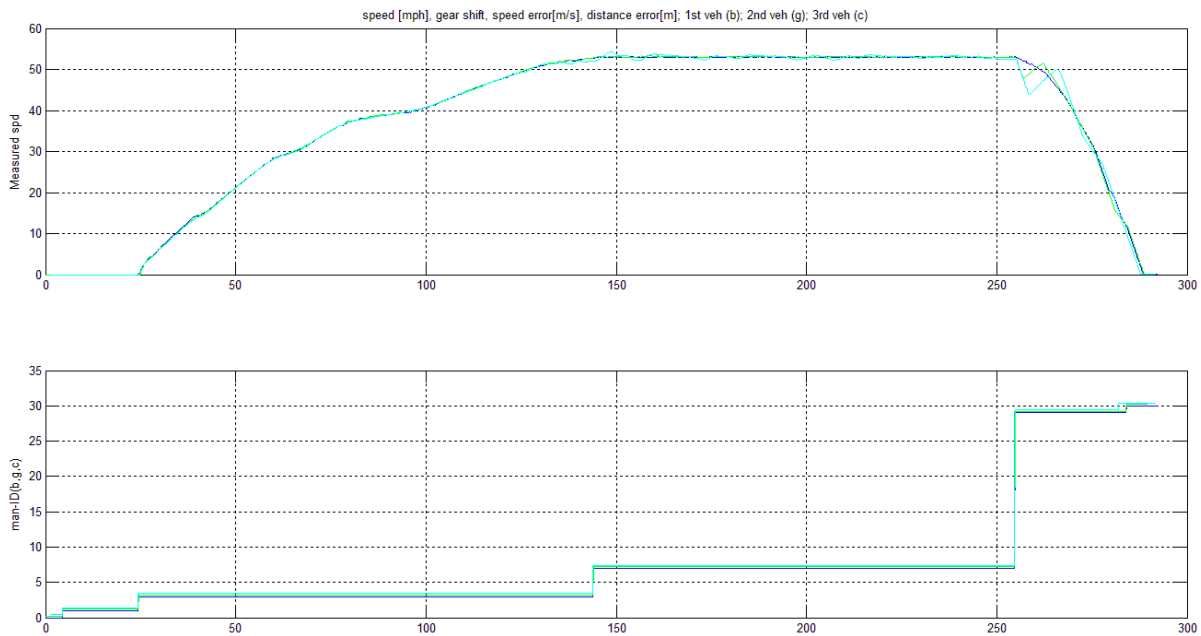


Figure 3.17. Ascending a hill with road grade indicated in Table 3.6 at 53 mph: speed measurement and maneuver ID

As can be observed from the upper plot, the two following vehicles (Gold and Silver trucks) were splitting a little at maneuver ID=29, which corresponds to the deceleration in preparation for a complete stop. When maneuver ID=30, open loop control of the air brakes was used to completely stop the vehicle. In most practical runs, this is the only time the air brake is actually used. In all other cases, the engine brake and transmission retarder were used for the limited deceleration needed to maintain platooning.

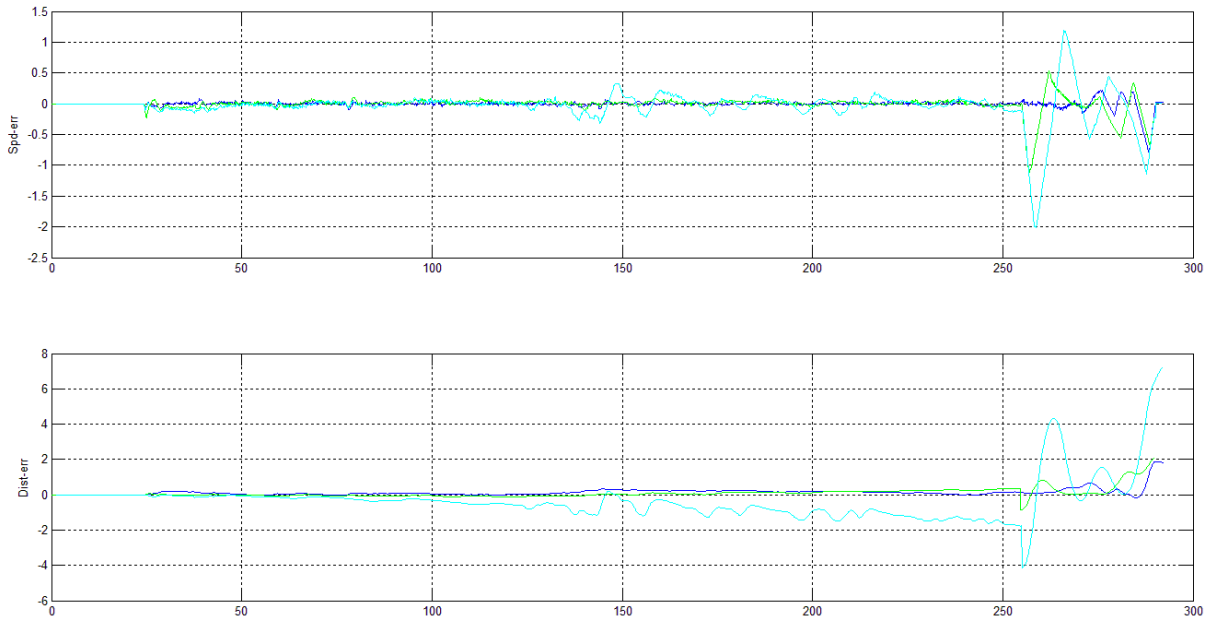


Figure 3.18. Ascending a hill with road grade indicated in Table 3.6 at 53 mph: speed tracking and distance tracking errors

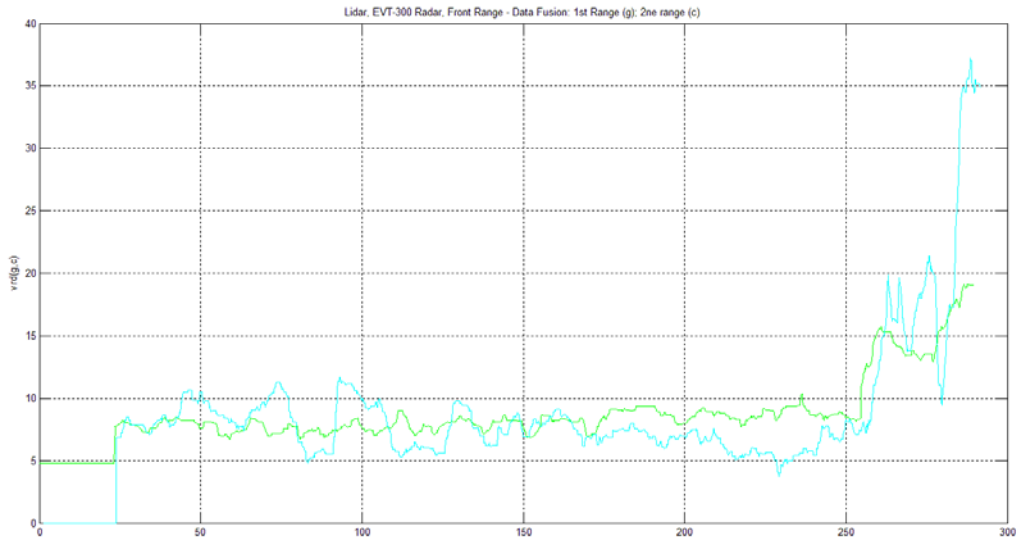


Figure 3.19. Ascending a hill with road grade indicated in Table 3.6 at 53 mph: EVT-300 radar measurement of the forward range

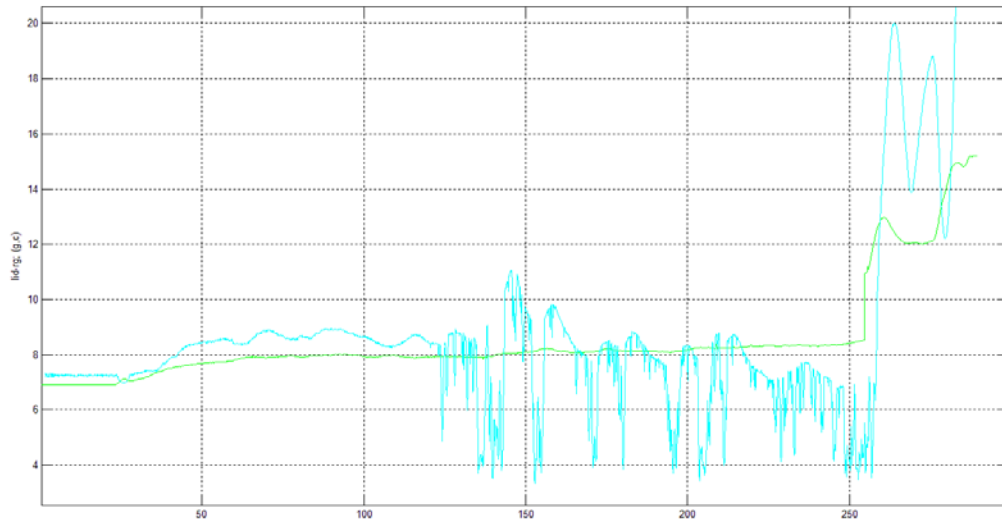


Figure 3.20. Ascending a hill with road grade indicated in Table 3.6 at 53 mph: lidar measurement of the forward range

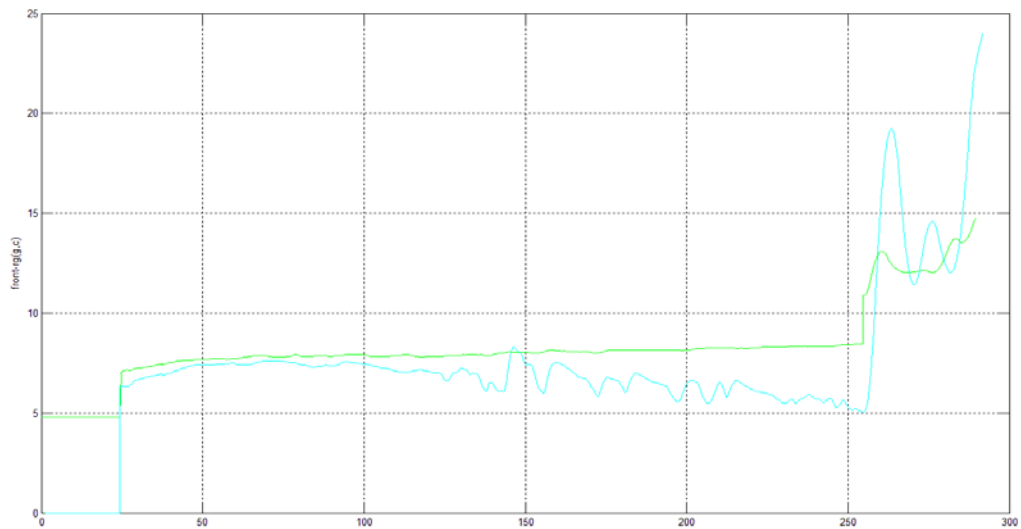


Figure 3.21. Ascending a hill with road grade indicated in Table 3.6 at 53 mph: fused forward range from radar and lidar

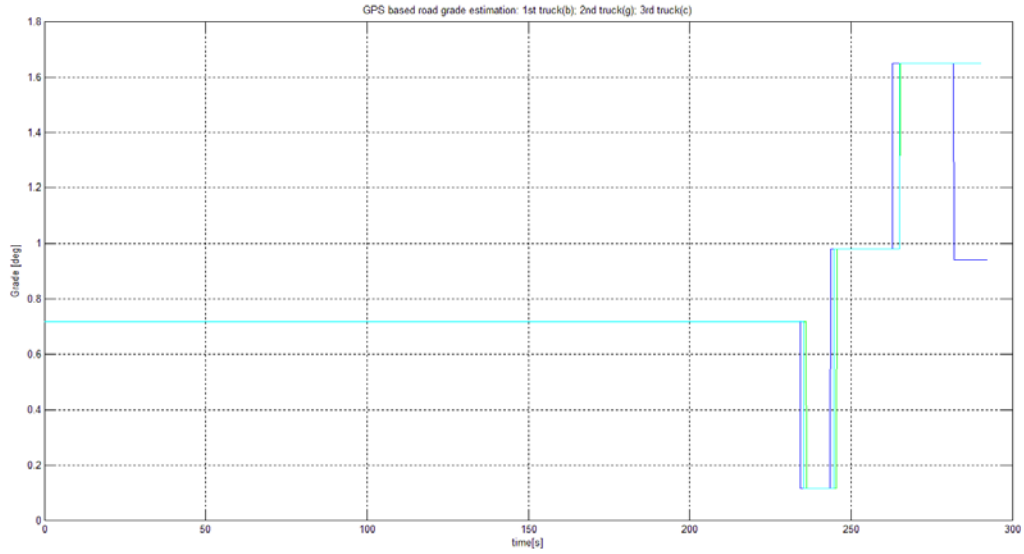


Figure 3.22 . Ascending a hill with road grade indicated in Table 3.6 at 53 mph: Road grade from GPS reading and lookup table

It is noted that the differences between the grade plots for the three trucks were caused by the different GPS coordinates of the locations of the three trucks.

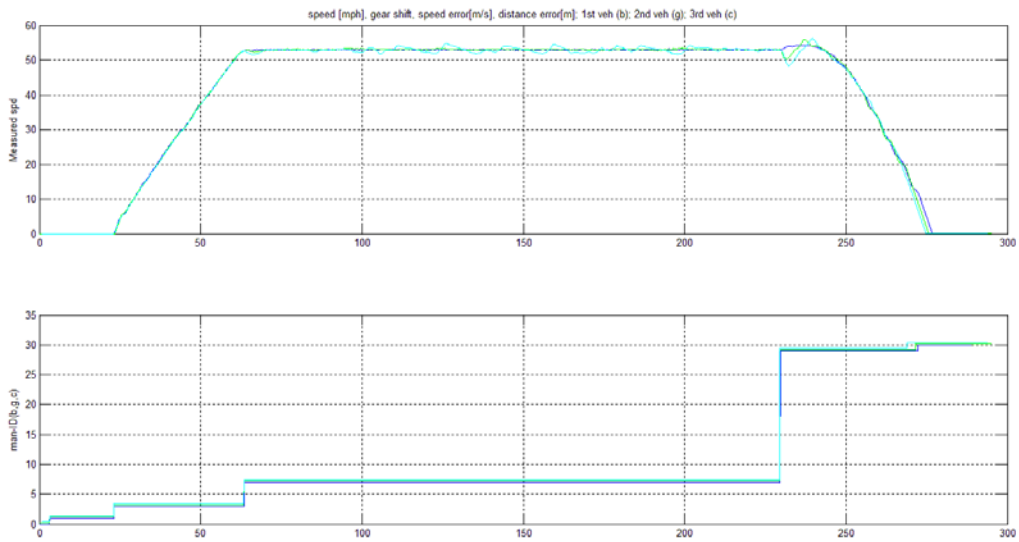


Figure 3.23. Descending a hill with road grade indicated in Table 3.6 at 53 mph: speed measurement and maneuver ID

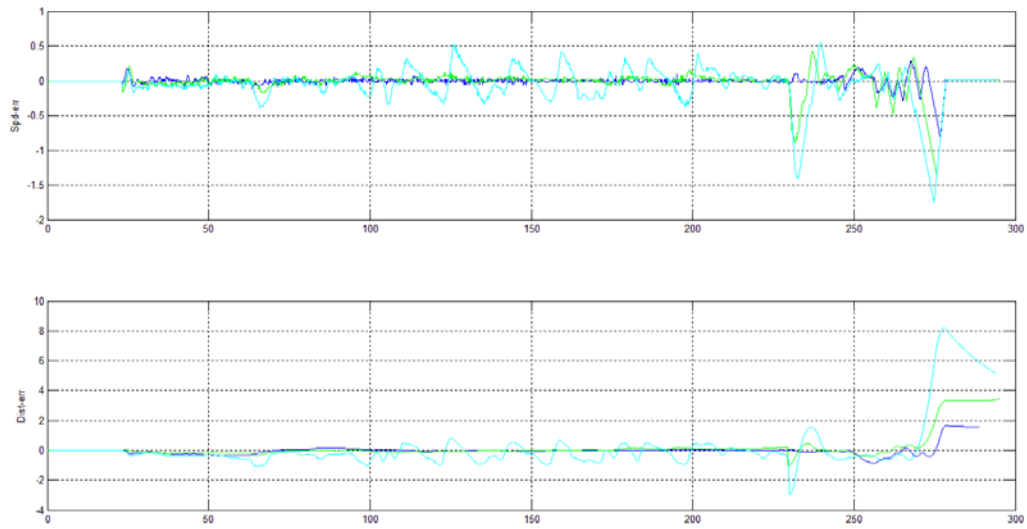


Figure 3.24. Descending a hill with road grade indicated in Table 3.6 at 53 mph: speed tracking and distance tracking errors

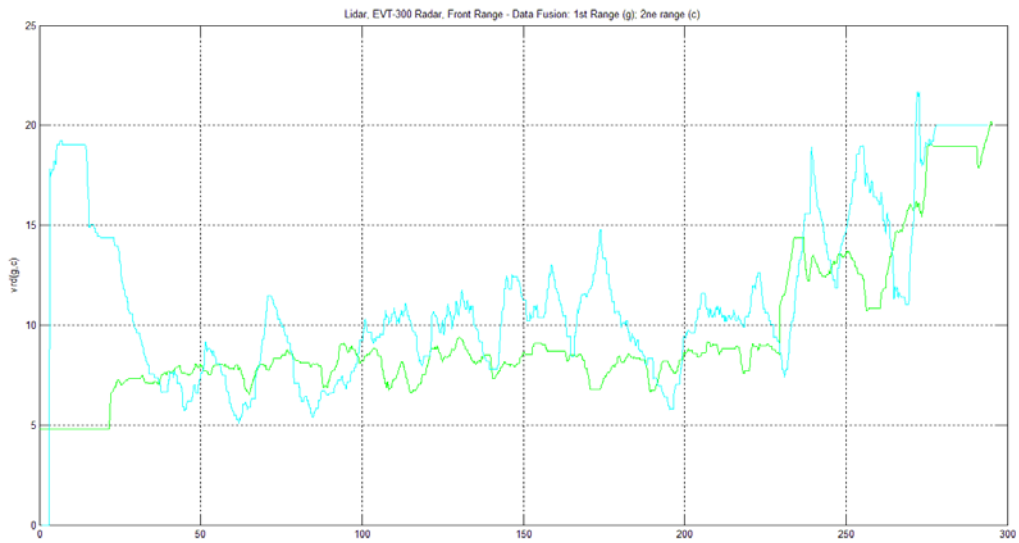


Figure 3.25. Descending a hill with road grade indicated in Table 3.6 at 53 mph: EVT-300 radar measurement of the forward range

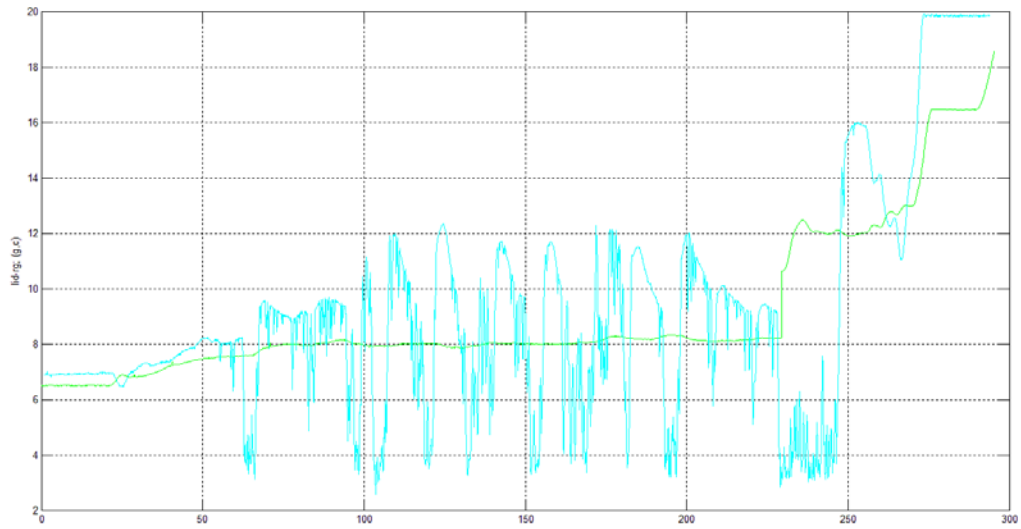


Figure 3.26. Descending a hill with road grade indicated in Table 3.6 at 53 mph: lidar measurement of the forward range

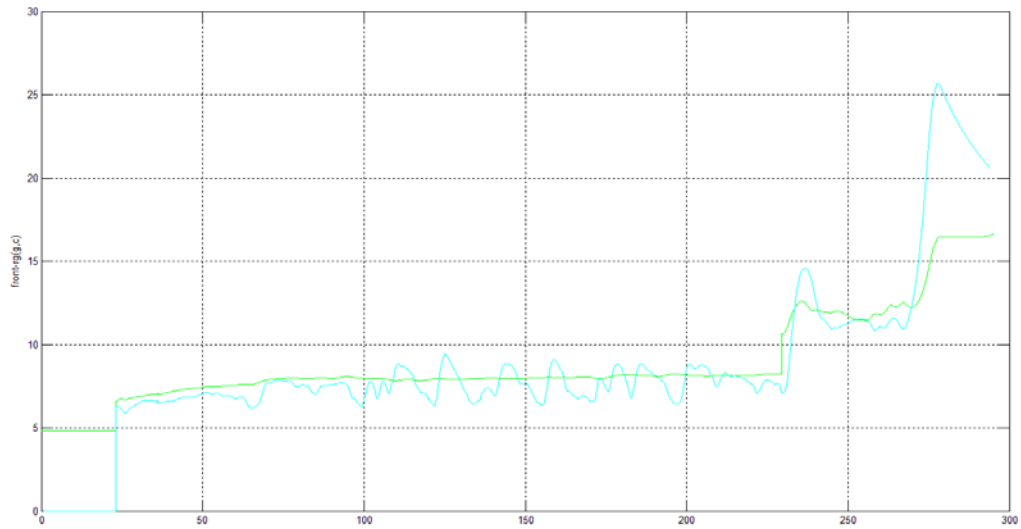


Figure 3.27. Descending a hill with road grade indicated in Table 3.6 at 53 mph: fused forward range from radar and lidar

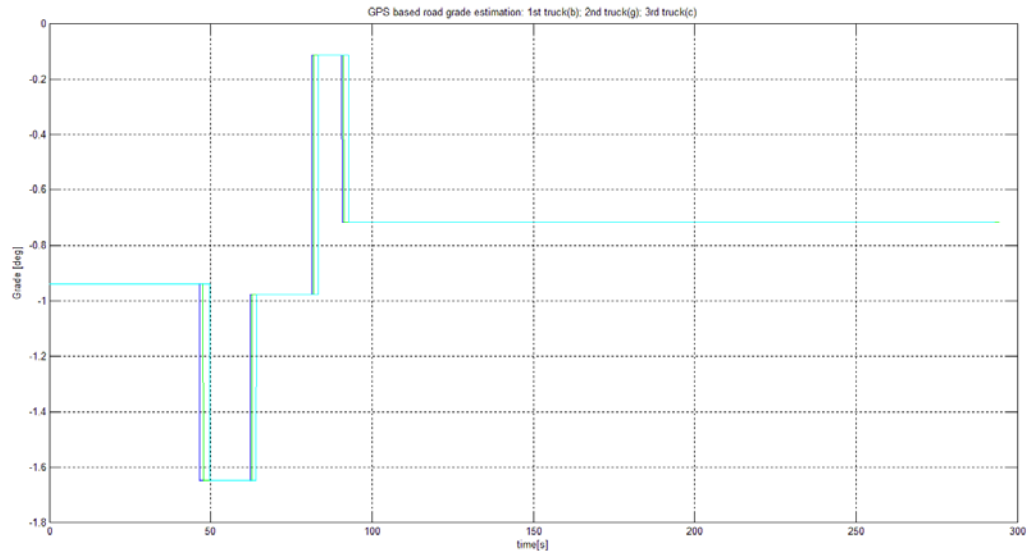


Figure 3.28. Descending a hill with road grade indicated in Table 3.6 at 53 mph: Road grade from GPS reading and lookup table

Table 3.7 RMS and Max Errors for Speed and Distance Tracking when Ascending and Descending a Hill.

Data number	Dir	Max spd [mph]	Des dist [m]	Blue – 1 st				Gold – 2 nd				Silver – 3 rd			
				Distance Error		Speed Error		Distance Error		Speed Error		Distance Error		Speed Error	
				RMS	Max	RMS	Max	RMS	Max	RMS	Max	RMS	Max	RMS	Max
101_9	Up	35	8	0.0893	0.1698	0.0139	0.0654	0.4946	1.4802	0.0275	0.0894	2.0061	3.2862	0.0296	0.1122
101_10	Down	35	8	0.1139	0.3912	0.0193	0.0870	0.4135	1.2258	0.0294	0.2130	0.6349	1.3752	0.0458	0.3342
102_12	Down	45	8	0.0733	0.3876	0.0154	0.0894	0.2123	0.6474	0.0322	0.2304	0.3029	1.1052	0.0797	0.3678
103_2	Up	50	8	0.0762	0.1662	0.0129	0.0672	0.1935	0.6432	0.0193	0.0846	0.4579	1.4064	0.0903	0.5886
103_3	Down	50	8	0.0383	0.3264	0.0193	0.1206	0.1728	0.5706	0.0338	0.1854	0.4232	1.2192	0.1298	0.4374
104_4	Up	53	8	0.1243	0.3336	0.0122	0.0792	0.2398	0.7272	0.0215	0.0864	0.7211	1.7724	0.0702	0.3312
104_5	Down	53	8	0.0470	0.2706	0.0180	0.1038	0.1612	0.6240	0.0368	0.1728	0.4189	1.0830	0.1491	0.5256
Mean				0.0803	0.2922	0.0159	0.0875	0.2697	0.8455	0.0286	0.1517	0.7093	1.6068	0.0849	0.3853

It can be observed that the distance tracking errors (both RMS and Max Error) for ascending and descending a hill are smaller than their counterparts for short distance platooning on the flat road. This can be explained as follows: the error for short distance following is mainly caused by drifting, which is essentially caused by the weight on the integral term in the controller. On a flat road, the external disturbance (from the road and the weather) was relatively small. Therefore, the offset kept accumulating. For grading up/down a hill, the disturbances from the road and from the weather (wind was stronger) are much larger. Such disturbances break the balance of the stiffness and force the controller to reset, which leads to a smaller distance tracking error.

4. Fault Detection and Handling

The fault detection and handling functions are implemented to improve safety of the truck platoon operations, to try to ensure that faults do not produce unsafe outcomes. The faults are classified in a simple hierarchy based on assumptions about their severity and the urgency of switching the trucks to a different mode of operation. The current fault detection and handling capability is rudimentary, just to improve safety during the testing and to alert the truck drivers and researchers working on the trucks about potentially unsafe conditions that they may not recognize immediately themselves. An operational system for use by normal truck drivers in their daily driving would need a much more comprehensive fault detection and handling system, capable of handling all possible fault conditions. Fault detection and handling for vehicle longitudinal control have been discussed in detail in [5].

The basic fault management strategies are:

- Level 1 faults: driver is alerted to take over control immediately;
- Level 2 faults: trucks will split to a longer distance and continue platooning;
- Level 3 faults: all three trucks will continue platooning unless another fault appears;

Fault Types	Diagnosis Method	Handling Priority	Handling Method
Computer system hardware	Message to DVI Watch-dog	1	Driver take over control
Computer operating system and application software	Message to DVI Watch-dog	1	Driver take over control
J-Bus reading	Longitudinal control: check: time stamp and/or value read	1	Driver take over control
J-Bus writing	Longitudinal control: check: its response	1	Driver take over control
Inter-vehicle communication	Longitudinal control: check count	1	Driver take over control
Longitudinal controller	Longitudinal control: actuators monitoring	1	Driver take over control
Remote Sensors: Both radar and Lidar	Longitudinal control: check tracking ID and distance	2	If both broken: use communication, vehicle speed, GPS; vehicle split

			and continue with longer following distance
Remote sensors: Radar or Lidar, but not both	Longitudinal control: check tracking ID and distance	3	Use one of radar or lidar combined with communication and GPS; continue platooning; but the driver needs to watch out

The determination of fault levels is based on the criticality of the component for control and string stability [2].

Indications Displayed on Driver-Vehicle Interface (DVI)

The DVI has four colored LEDs used to display system status (**Green**, **Amber**, **Red** and **Blue**):

- At Initial start-up time:
 - **Green**: driver pressed the Auto button to initiate automated operation and system readings are OK; but the communication handshake is not yet established with the other trucks;
 - **Red**: Manual Mode; driver did not press the button and/or the system has some initial problem;
 - **Blue**: Communication handshake ON
 - **Green & Blue**: Communication handshake ON and system is fine and ready to go;
- After Starting Period – On the move for fault detection display
 - **Red + Beeping (Noise)**: Priority 1 (Hard Fault(s)) Fault Handling, driver must take over immediately
 - **Green + Flashing Yellow**: Priority 2 Fault Handling (Medium Fault(s)), system automatic handling by splitting platoon and slowing vehicles down to stop
 - **Green + Steady Yellow**: Priority 3 Fault Handling (Minor Fault(s)), system automatic handling, platooning continues; but driver needs to watch over the system to be prepared to take over;
 - **Green**: System healthy
 - **No LED + Beeping** – driver needs to take over immediately due to computer or power failure.

5. Fuel Economy Analysis

Energy saving through reduction of aerodynamic drag is one of the most important expected benefits from close-formation automated platoon driving, so it is important to understand how much energy could be saved under different conditions. The key variables investigated here were the effects of the position within the platoon and the inter-vehicle spacing. All tests were conducted at a single speed, since the dependence of aerodynamic drag on speed is a well-known quadratic relationship. The test site was at an altitude of 6000 ft (1800 m), where the air density is only 80% of the density at sea level. This means that the drag savings should be expected to be significantly larger at sea level.

5.1 Vehicles and Trailers

The three trucks used for the tests were the same model, with the same engine horsepower rating. The three trailers rented for each test (September 2010 and May 2011) were identical for all three trucks. However, the trailers in the two tests were from different manufacturers although they were all 53 feet long. This means that they could be different in weight and rolling resistance and could lead to slightly different aerodynamic effects. Therefore, the test results from September 2010 and May 2011 cannot be compared directly.

The first and second trailers were equipped with a reflector at their rear surfaces, hiding the rear axle and tires and mud flaps to enhance lidar and radar detection and ensure that their beams were always reflecting off the same surface at the rear edge of the trailer body. As shown in Figure 5.1, it was made of a plywood board covered with a metallic reflecting sheet and was about the width of the trailer and about 1.2 feet high. The weight of the reflector can be ignored compared to the weight of the trailer. Since the reflector is mounted behind the rear wheels, its contribution to aerodynamic drag has also been considered small and ignored.



Figure 5.1. Reflector to help lidar and radar detection behind and underneath the trailer.

5.2 Test Environment and the Weather

The weather conditions for the two series of tests were quite different. For the tests in September 2010, the weather was very mild and there was almost no wind. However, the wind was very strong almost every afternoon for the tests in May 2011 – the temperature was reasonably mild but the wind began to pick up from around lunch time and gradually grow in strength in the afternoon. We set up a weather station at one end of the test site to monitor the general ambient conditions. Since the test section was 5 miles long, and the update rate of the weather station data was every 30 minutes, we could not distinguish the wind direction and intensity for each individual run, but rather gained a general description of the conditions. The following Table 5.1 shows the wind intensity and the direction recorded on May 27 when most of the three truck platooning was tested.

In Table 5.1, the wind speed is the average speed for the past 30 minutes; high speed is the highest wind speed recorded in the last 30 minutes in the highest speed direction. It can be observed that

- the unit for wind speed is mph
- wind speed is not consistent in time
- wind direction is not consistent in time
- wind was stronger in the afternoon than in the morning

It can be observed from Figure 2.4 that the trucks driving along the test section on SR722 would be facing either Northeast (NE) or Southwest (SW). All the winds had components crossing the

vehicle motion direction, but the prevailing westerly direction of the winds meant that the test runs heading southwest had a significant headwind component while the runs in the opposite direction had a significant tailwind component.

Table 5.1. Wind intensity and directions recorded by the weather station near the west end of the test section on SR722 at Austin, Nevada.

Date	Time	Temp Out	Wind Speed	Wind Dir	Highest Speed	High Speed Dir
5/27/2011	9:00 AM	55.1	6	W	13	WSW
5/27/2011	9:30 AM	54.3	6	W	12	SW
5/27/2011	10:00 AM	55.9	5	W	12	W
5/27/2011	10:30 AM	55.5	6	W	13	WSW
5/27/2011	11:00 AM	56.7	6	WNW	14	W
5/27/2011	11:30 AM	57.1	8	W	17	SW
5/27/2011	12:00 PM	57.3	8	W	15	WSW
5/27/2011	12:30 PM	58.2	8	WNW	18	WNW
5/27/2011	1:00 PM	60.3	8	WNW	17	NW
5/27/2011	1:30 PM	61.3	8	WNW	17	NW
5/27/2011	2:00 PM	63.8	8	WNW	17	WNW
5/27/2011	2:30 PM	62.9	10	W	21	W
5/27/2011	3:00 PM	61.1	9	WNW	18	W
5/27/2011	3:30 PM	60.1	10	NW	16	W
5/27/2011	4:00 PM	62.4	11	NW	18	WNW
5/27/2011	4:30 PM	61.3	10	NW	19	WNW
5/27/2011	5:00 PM	60.3	9	NW	18	N
5/27/2011	5:30 PM	68.5	3	NW	18	NW

5.3 Effect of Inter-vehicle Distance on Fuel Economy

For the tests in September 2010, the shortest inter-vehicle distance was 6 m and the truck sequence in the platoon was Blue, Gold and then Silver, so in order to be consistent with that set of data (described in Section 5.5), the same sequence of trucks was used to analyze the effect of inter-vehicle distance on fuel economy in the May 2011 tests. These tests were conducted mostly in the morning of May 27, 2011. As indicated in Table 5.1, the wind effect was relatively small in the morning of May 27.

To eliminate the direction effect, both in wind direction and in road geometry (since WB has a slight up grade), we separated the data from the WB and EB runs. The units for the Distance mean fuel consumption are: gram/mile and for Time mean fuel consumption gram/minute.

Table 5.2. Distance Mean fuel consumption [grams/mile] and Time Mean fuel consumption [grams/minute] in cruising phase (at speed 53 mph – 87 km/h) for the platoon configuration Blue, Gold, Silver:

Data No.	Dir	Max speed [mph]	Follow distance [m]	Blue – 1 st		Gold – 2 nd		Silver – 3 rd	
				Dist Mean	Time Mean	Dist Mean	Time Mean	Dist Mean	Time Mean
02_13	W	53	8	608	537	596	527	591	522
02_15	E	53	8	488	431	492	435	488	431
03_16	W	53	7	684	604	641	567	620	547
03_17	E	53	7	456	403	414	366	434	383
04_07	W	53	6	614	542	591	522	620	547
04_08	W	53	6	623	550	600	531	594	525
04_09	E	53	6	440	389	428	378	422	372
05_10	W	53	5	614	542	585	517	566	500
05_11	E	53	5	428	378	412	365	436	385
05_12	W	53	5	649	573	602	532	620	547
05_13	E	53	5	398	351	382	338	402	355
06_14	W	53	4	611	539	562	496	584	515
06_15	E	53	4	443	391	413	365	429	378
06_3	E	53	4	388	343	366	324	357	315
06_4	W	53	4	599	529	565	499	574	507
06_5	E	53	4	365	322	346	305	343	303

Now we separate the data table into EB and WB and average the fuel consumption at the same speed and distance for EB and WB respectively. The following tables are obtained:

Table 5.3. Fuel consumption for Eastbound test runs with the data for each inter-vehicle distance aggregated from Table 5.2.

Dir	Max speed [mph]	Follow distance [m]	Blue – 1 st		Gold – 2 nd		Silver – 3 rd	
			Dist mean	Time mean	Dist mean	Time mean	Dist mean	Time mean
E	53	8	488	431	492	435	488	431
E	53	7	456	403	414	366	434	383
E	53	6	440	389	428	378	422	372
E	53	5	413	365	397	351	419	370
E	53	4	399	352	375	331	376	332

Note that in Table 5.3, the third and fifth rows are aggregated from multiple runs in Table 5.2.

Table 5.4. Fuel consumption for Westbound runs with the data for each inter-vehicle distance aggregated from Table 5.2.

Dir	Max speed [mph]	Follow distance [m]	Blue – 1 st		Gold – 2 nd		Silver – 3 rd	
			Dist mean	Time mean	Dist mean	Time mean	Dist mean	Time mean
W	53	8	608	537	596	527	591	522
W	53	7	684	604	641	567	620	547
W	53	6	618	546	596	527	607	536
W	53	5	631	558	593	525	593	523
W	53	4	605	534	563	498	579	511

Note that the third, fourth and fifth rows are aggregated from multiple runs in Table 5.2.

From Tables 5.3 and 5.4, it can be observed that:

- (1) for both eastbound and westbound test runs, fuel consumption decreases as inter-vehicle distance decreases;
- (2) the position effect with a platoon: it is clear that the first truck consumes more fuel than the second and the third trucks; however, the fuel consumption differences between the second and third trucks here are not significant.

5.4 Comparison with Single Truck Runs

Test data from runs on May 23 have been used to estimate fuel consumption of single trucks at a cruise speed of 53 mph.

Table 5.5 Time mean fuel consumption [grams/minute] and distance mean fuel consumption [grams/mile] at cruising phase (at the maximum speed 53 mph) for individual runs of the three test trucks.

Data number	Dir	Cruise speed [mph]	Blue		Gold		Silver	
			Dist mean	Time mean	Dist mean	Time mean	Dist mean	Time mean
22_3	E		484	428	492	435	553	489
22_4	W		570	504	564	498	567	501
Mean			527	466	528	466	560	495

Table 5.6 Ratios of time mean and distance mean fuel consumption of the trucks in platoon following to the same trucks driven independently

Dir	Max speed [mph]	Follow distance [m]	Blue – 1 st		Gold – 2 nd		Silver – 3 rd	
			Dist mean ratio	Time mean ratio	Dist mean ratio	Time mean ratio	Dist mean ratio	Time mean ratio
W	53	8	1.066	1.066	1.057	1.057	1.042	1.042
W	53	7	1.199	1.199	1.137	1.138	1.093	1.092
W	53	6	1.084	1.084	1.056	1.057	1.071	1.070
W	53	5	1.107	1.107	1.052	1.053	1.046	1.045
W	53	4	1.060	1.060	0.999	0.999	1.021	1.020
E	53	8	1.007	1.007	1.001	1.001	0.882	0.882
E	53	7	0.942	0.942	0.841	0.842	0.784	0.784
E	53	6	0.908	0.908	0.870	0.870	0.762	0.762
E	53	5	0.853	0.853	0.808	0.808	0.758	0.758
E	53	4	0.823	0.823	0.762	0.762	0.680	0.679

These results show a dramatic contrast based on direction of travel, which has to be associated with the ambient wind conditions at the time of these test runs, with their strong component from the West. The westbound platoon test runs show fuel consumption higher than the baseline for the individual trucks, with relatively little difference based on position within the platoon or the following distance. The westbound test run at a following distance of 7 m showed conspicuously

high fuel consumption for all trucks, implying that it was done with the strongest headwind. In contrast, the eastbound platoon runs with tailwinds show strong effects on fuel consumption based on both following distance and the position of the truck within the platoon.

Comparing the eastbound results at the 8 m gap and 4 m gap, we see the lead truck reducing its fuel consumption by about 18%, while the second truck saved 24% and the third truck saved 23%, indicating potentially large improvements from shortening the gap. However, these results cannot be extrapolated to more general conditions because of the same confounding effect of the ambient winds that implied virtually no effect of gap changes on the westbound runs.

5.5 Effect of Vehicle Position in a Platoon

The tests in September 2010 on the same section of roadway had multiple runs at 6 m following distance and the weather was very mild, with almost no wind at all. These data have been used for a preliminary analysis of the effect of truck position on fuel consumption.

Table 5.7. Distance Mean and Time Mean fuel consumption for Eastbound three truck platooning runs at 53 mph;

Data number	Dir	Max speed [mph]	Follow dist [m]	Blue – 1 st		Gold – 2 nd		Silver – 3 rd	
				Dist mean	Time mean	Dist mean	Time mean	Dist mean	Time mean
2_2	E	53	6	464	410	398	352	400	354
2_4	E	53	6	439	387	403	356	387	342
2_6	E	53	6	437	386	409	362	375	331
2_8	E	53	6	420	371	405	358	373	329
Mean	E	53	6	439.8	388.5	404.0	356.9	383.7	339.0

Table 5.8. Distance Mean and Time Mean fuel consumption for Westbound three truck platooning at 53 mph;

Data number	Dir	Max speed [mph]	Follow dist [m]	Blue – 1 st		Gold – 2 nd		Silver – 3 rd	
				Dist mean	Time mean	Dist mean	Time mean	Dist mean	Time mean
2_1	W	53	6	554	490	555	490	500	442
2_3	W	53	6	550	486	516	456	494	437
2_5	W	53	6	543	480	516	456	501	443
2_7	W	53	6	541	478	517	457	493	436
Mean	W			547.2	483.3	526.1	464.8	497.2	439.3

It can be observed in Tables 5.7 and 5.8 that, both Distance Mean and Time Mean fuel consumption shows the position effect: the second truck saves fuel compared to the first truck,

and the third truck saves even more compared to the second truck. It is noted that these fuel consumption results are somewhat distorted because of the way we drove the second vehicle. The three trucks were not perfectly aligned laterally because we had only one wireless antenna for each truck, so to avoid radio signal dropouts, we intentionally drove the second truck offset to the left side (closer to the center line). This affected the aerodynamic drag on both the second and third trucks in the platoon. If all the trucks were driven in perfect alignment, the fuel consumption reduction would have been more significant for the second vehicle.

Table 5.9. Distance Mean (g/mile) and Time Mean (g/minute) fuel consumption of three truck WB individual runs at 53 mph.

Data number	Dir	Max speed [mph]	Blue – 1 st		Gold – 2 nd		Silver – 3 rd	
			Dist mean	Time mean	Dist mean	Time mean	Dist mean	Time mean
2_1	W	53	586	517	578	511	569	502
2_3	W	53	582	514	584	516	560	494
2_5	W	53	585	517	582	514	541	478
Mean			584.3	516.1	581.4	513.6	556.4	491.4
2_2	E	53	456	403	456	403	474	419
2_4	E	53	459	405	473	418	436	385
2_6	E	53	433	382	432	381	442	442
Mean			449.3	396.9	453.8	400.8	450.8	415.4

Table 5.10. Ratios of fuel consumption for platooning at 6 m gap compared to individual truck runs, without wind influence

Data number	Dir	Max speed [mph]	Follow dist [m]	Blue – 1 st		Gold – 2 nd		Silver – 3 rd	
				Dist mean ratio	Time mean ratio	Dist mean ratio	Time mean ratio	Dist mean ratio	Time mean ratio
2_1	W	53	6	0.949	0.949	0.954	0.954	0.899	0.899
2_3	W	53	6	0.942	0.942	0.888	0.888	0.889	0.889
2_5	W	53	6	0.930	0.930	0.888	0.889	0.900	0.901
2_7	W	53	6	0.926	0.926	0.890	0.890	0.887	0.887
Mean	W	53	6	0.9365	0.9365	0.9049	0.9051	0.8937	0.8939
2_2	E	53	6	1.032	1.032	0.878	0.878	0.887	0.851
2_4	E	53	6	0.976	0.976	0.888	0.888	0.859	0.823
2_6	E	53	6	0.973	0.973	0.902	0.902	0.831	0.797
2_8	E	53	6	0.935	0.935	0.894	0.894	0.827	0.793
Mean	E	53	6	0.9790	0.9790	0.8903	0.8904	0.8510	0.8161
Mean	E+W	53	6	0.9577	0.9577	0.8976	0.8978	0.8723	0.8550

The mean value results for both directions of travel indicate that the lead truck saves about 4.2% in fuel consumption when the others follow it in platoon formation at 6 m gap. The second truck saves about 10% and the third truck saves 13% to 14.5%.

For the truck fuel consumption analysis, the *Accumulated Fuel Consumption* (AFC) for each truck in the following scenarios was measured:

- single truck individual runs
- three truck platooning at 6 m gap

The AFC is obtained by integration of the fuel consumption rate for each vehicle individually during the cruising phase, when the reference speed of the platoon is constant. These results are shown graphically in Figure 5.2, averaging the results from eight runs (four in each direction). These results show that:

- (1) The lead vehicle has the highest fuel consumption of the three;
- (2) The second vehicle consumed 6% less fuel than the leader, and the third vehicle consumed 11% less than the leader when platooned at 6 m gap.
- (3) The fuel consumption rates of each truck in the platoon at 6 m gaps compared to single truck runs by the same trucks are:
 - First truck fuel reduction: 4.3%
 - Second truck fuel reduction: 10%
 - Third truck fuel reduction: 14%

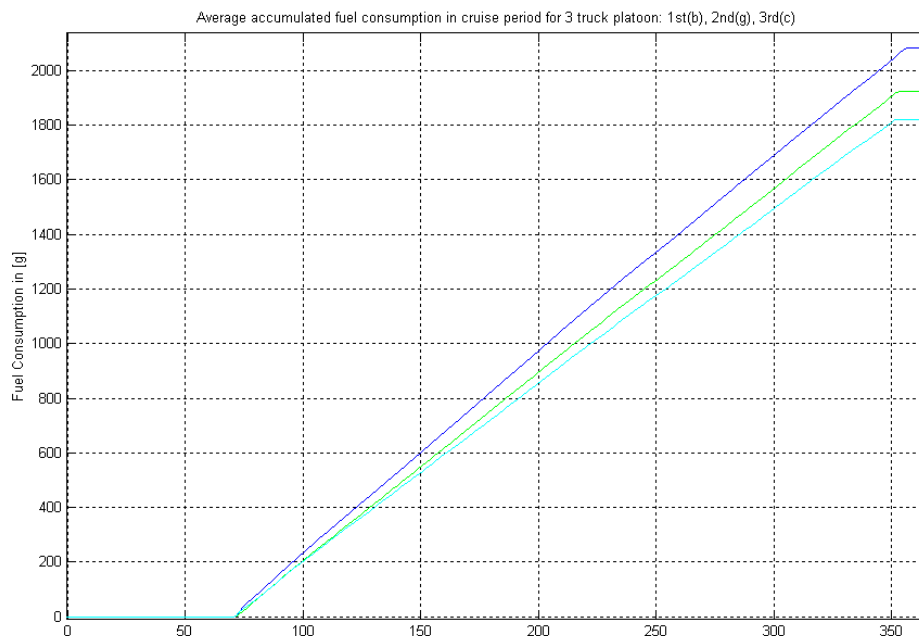


Figure 5.2. Average Accumulated Fuel Consumption of Three Trucks in Platoon at 6 m Spacing

The carefully controlled 2003 measurements on a two-truck automated truck platoon reported by Browand, McArthur and Radovich [8] indicated that at the 6 m gap, the front truck would save 7% and the following truck would save 9% compared to their fuel consumption when driven individually. By comparison, the more recent three-truck tests indicate a smaller reduction in the fuel saving by the front truck, but a significant improvement in the fuel saving by the following trucks. This improvement in the following truck fuel consumption is attributable to the extension from two trucks to three trucks in the platoon.

6. Concluding Remarks

The automated truck platoon tests demonstrated several important results:

- (a) The DSRC communication system at 5.9 GHz, with 100 ms update intervals, has sufficient capabilities to support this most demanding of V2V communication applications. Two different generations of DSRC transceivers were used on the test trucks at different times, the Savari Onboard Units (SOBU) and the Denso Wireless Safety Units (WSU). The Denso WSUs have the advantage that they implement more of the IEEE 1609 standards, including diversity, but although they worked well for low-speed testing of the truck-tractors at the Richmond Field Station, they failed to work for high-speed highway testing with 53-ft trailers in central Nevada. This was disappointing because their diversity capability was seen as an important feature in enabling the first and third trucks to maintain line of sight contact under all road conditions, including curves and grade changes, without requiring lateral offset of the second truck.
- (b) A platoon of three tractor-trailer trucks was successfully driven under automated longitudinal platoon control, maintaining adequate tolerances on longitudinal gap variations while cruising and maneuvering. On an essentially flat section of road, the rms error in vehicle-following gap was maintained within 0.9 m and the maximum error was maintained within 1.6 m for the second truck following the first while cruising at a steady speed of 85 km/h. The analogous values for the third truck following the second were 1.2 m and 2.1 m (Table 2.4).
- (c) The truck platoon was tested for a range of target inter-truck following gaps, beginning with 10 m. As the performance at each gap was verified to be satisfactory, shorter gaps were attempted, going as short as a 4 m gap by the end of the testing period. These results show the basic technical feasibility of closely-coordinated longitudinal control of heavy trucks in a platoon, maintaining short gaps using the combination of DSRC radio communications and radar and lidar ranging sensors.
- (d) The DSRC radios were also used to coordinate maneuvers among the trucks, with a particular focus on platoon joining and splitting maneuvers. These maneuvers were performed in

different combinations, simultaneously and sequentially for the joins and splits between the first and second and the second and third trucks. The sequential maneuvers are to be preferred for future implementations because the simultaneous maneuvers require significantly larger speed changes by the third truck. The platoon joining from a 14 m gap to a 10 m gap required 35 seconds of transition time, and the splitting from 10 m to 14 m gap required 25 seconds of transition time.

(e) The trucks were also maneuvered through a sequence of speed profile changes to test the ability of the following trucks to follow the leader. The rate of speed changes for these maneuvers had to be limited based on the curve in Figure 3.6 because of the fundamental power limitations of the trucks. The speed change tests showed that the second truck followed the first with an effective lag of 0.8 seconds, and the third truck followed with an effective lag of 1.2 seconds relative to the first. The rms errors in gap and speed between the trucks throughout the speed change tests were 0.22 m and 0.01 m/s (average) and 0.57 m/s (max) between the first and second trucks and 0.25 m and 0.07 m/s (average) and 0.65 m/s (max) between the second and third trucks (Table 3.1).

(f) One of the largest potential benefits from truck platooning is the saving of energy and CO₂ emissions based on reductions in aerodynamic drag. The direct fuel consumption of the trucks was monitored throughout the testing through their engine controllers' fuel injection systems, and the trends in fuel consumption were studied to provide initial estimates of the benefits that could be gained. These measurements are difficult to control carefully because of the strong influence of wind conditions on the drag. Although the September 2010 tests were conducted under calm winds, the May 2011 tests suffered from strong wind conditions, and the tight schedule compelled the project team to use all available time for testing, including the strong wind times, which produced noisier results than we would have preferred.

All the trucks in the platoon save fuel when they are driven at close spacing within the platoon. The lead truck saves less than the followers save, and there is some inconsistency in the results regarding the savings by the second and third trucks. Nevertheless, we should expect the first truck in a platoon at 6 m gaps to be able to save 4.3% of its normal fuel consumption in steady cruising on flat roads at 85 km/h, with the following trucks saving 10% to 14%. Because these results were measured at an altitude of 6000 ft. (1800 m), where the air density is only 80% of that at sea level, the relative savings at sea level should be more significant since the total aerodynamic drag should be about 25% higher than it was at the high-altitude test site (while the other losses would be unchanged).

When we consider that many long-distance trucks in the U.S. cruise at speeds around 115 km/h (71 mph) rather than the 85 km/h speed of these tests, their aerodynamic drag could be 80% higher than we measured since the drag increases with the square of the speed. Combining this effect with the altitude effect, the typical aerodynamic drag experienced by trucks operating in long-distance revenue service could be twice as high as it was in our tests. Following the rule of

thumb that aerodynamic drag accounts for about half of fuel consumption of trucks at highway speed, this implies that the fuel savings that would be experienced in practice could be 50% higher than what we measured in these tests.

These results show strong enough potential fuel savings to justify significantly more attention to truck platooning in the future, as we become increasingly concerned about how to reduce consumption of petroleum-based fuels.

(g) A limited fault detection and identification system was implemented on the experimental trucks to provide visible indicators to the truck driver and the researcher observing from the passenger seat about the status of the truck control system, so that they would be made aware of potential problems as soon as possible. This was found to be particularly important and useful for faults on one truck that may not otherwise be apparent to people traveling in another truck with which it is closely coupled.

7. References

- [1] X. Y. Lu and J. K. Hedrick, 2002, Modeling of Heavy-Duty Vehicles for Longitudinal Control, *The 6th Int. Symposium on Advanced Vehicle Control*, Hiroshima, Japan, Sept. 9-13, Paper No. 109
- [2] X. Y. Lu and J. K. Hedrick, 2002, A Panoramic View of Fault Management for Longitudinal Control of Automated Vehicle Platooning, *Proc. of the 2002 ASME Congress*, Nov. 17-22, New Orleans
- [3] X. Y. Lu and J. K. Hedrick, 2003, Longitudinal Control Design and Experiment for Heavy-Duty Trucks, *Proc. of 2003 American Control Conference*, June 4-6, Denver, Colorado, USA
- [4] X. Y. Lu and K. Hedrick, 2004, Practical String Stability for Longitudinal Control of Automated Vehicles, *Int. J. of Vehicle Systems Dynamics Supplement, Vol. 41*, p577-586
- [5] X. Y. Lu, S. Shladover and J. K. Hedrick, 2004, Heavy-Duty Truck Control: Short Inter-Vehicle Distance Following, *Proc. of 2004 American Control Conference, (ACC-04)*, June 30 - July 2, Boston, MA
- [6] X. Y. Lu and J. K. Hedrick, Heavy-Duty Vehicle Modeling and Longitudinal Control, *Int. J. of Vehicle Systems Dynamics, Vol. 43, No. 9*, Sept. 2005, pp.653-669
- [7] S. Shladover, X. Y. Lu, B. Song, S. Dickey, C. Nowakowski, A. Howell, F. Bu, D. Marco, H. Tan, and D. Nelson, (2005). Demonstration of Automated Heavy-Duty Vehicles, **UCB-ITS-PRR-2005-23**, Berkeley, CA: California PATH Program, Institute of Transportation Studies, University of California, Berkeley
- [8] F. Browand, J. McArthur and C. Radovich, "Fuel Saving Achieved in the Field Test of Two Tandem Trucks, PATH Research Report UCB-ITS-PRR-2004-20.
- [9] X. Y. Lu, S. Shladover, and J. Hedrick, Longitudinal transition control for Heavy-Duty Trucks: between manual and automatic, *Proc. 15th ITS World Congress*, November 16-20, 2008, New York